THE JOURNAL OF BIOLOGICAL CHEMISTRY VOL. 289, NO. 47, pp. 32757–32772, November 21, 2014

Toll-like Receptors as a Target of Food-derived Anti-inflammatory Compounds*[S]

Received for publication, June 4, 2014, and in revised form, October 6, 2014 Published, JBC Papers in Press, October 7, 2014, DOI 10.1074/jbc.M114.585901

Takahiro Shibata[‡1], Fumie Nakashima[‡1], Kazuya Honda[‡1], Yu-Jhang Lu[‡], Tatsuhiko Kondo[‡], Yusuke Ushida[§], Koichi Aizawa[§], Hiroyuki Suganuma[§], Sho Oe[¶], Hiroshi Tanaka[¶], Takashi Takahashi[¶], and Koji Uchida[‡2]

From the [‡]Graduate School of Bioagricultural Sciences, Nagoya University, Nagoya 464-8601, Japan, [§]Research and Development Division, Kagome Company, Limited, 17 Nishitomiyama, Nasushiobara 329-2762, Japan, and [¶]Graduate School of Science and Engineering, Tokyo Institute of Technology, Tokyo 152-8552, Japan

Background: Vegetable-rich diets are associated with the reduced risk of inflammatory diseases.
Results: Iberin, an isothiocyanate compound from cabbage, targeted TLRs, disrupted TLR dimerization, and inhibited the inflammatory responses.
Conclusion: The TLR dimerization step is a target of food-derived anti-inflammatory compounds.
Significance: These findings extend our understanding of how isothiocyanates show their medical benefits as anti-inflammatory food components.

Toll-like receptors (TLRs) play a key role in linking pathogen recognition with the induction of innate immunity. They have been implicated in the pathogenesis of chronic inflammatory diseases, representing potential targets for prevention/treatment. Vegetable-rich diets are associated with the reduced risk of several inflammatory disorders. In the present study, based on an extensive screening of vegetable extracts for TLR-inhibiting activity in HEK293 cells co-expressing TLR with the NF-κB reporter gene, we found cabbage and onion extracts to be the richest sources of a TLR signaling inhibitor. To identify the active substances, we performed activity-guiding separation of the principal inhibitors and identified 3-methylsulfinylpropyl isothiocyanate (iberin) from the cabbage and quercetin and quercetin 4′-*O*-β-glucoside from the onion, among which iberin showed the most potent inhibitory effect. It was revealed that iberin specifically acted on the dimerization step of TLRs in the TLR signaling pathway. To gain insight into the inhibitory mechanism of TLR dimerization, we developed a novel probe combining an isothiocyanate-reactive group and an alkyne functionality for click chemistry and detected the probe bound to the TLRs in living cells, suggesting that iberin disrupts dimerization of the TLRs via covalent binding. Furthermore, we designed a variety of iberin analogues and found that the inhibition potency was influenced by the oxidation state of the sulfur. Modeling studies of the iberin analogues showed that the oxidation state of sulfur might influence the global shape of the isothiocyanates. These findings establish the TLR dimerization step as a target of food-derived anti-inflammatory compounds.

Inflammation, induced by tissue injuries and microbial infection, is one of the most organized biological processes. A major trigger of the inflammatory response is the recognition of microbe-associated molecular patterns by specific receptors of the innate immune system that play a critical role in the induction of early signals initiating and establishing the inflammatory setting (1). A primary function of inflammation is the resolution of infection and repair of the damage to maintain homeostasis. Thus, the ideal inflammatory response is rapid and destructive but specific and self-limiting (2). The importance of this balance is demonstrated by the findings in certain chronic infectious or inflammatory disorders that the inflammatory response causes more damage to the host than the microbe. Inflammation and the immune system are intimately tied together. Indeed, an overactivation of the innate immune response can cause chronic inflammation due to inefficient regulation of the inflammatory responses (3). Inflammation provides a unifying pathophysiological mechanism underlying many chronic disorders, including diabetes, cardiovascular disease, certain cancers, bowel diseases, arthritides, and osteoporosis.

Toll-like receptors (TLRs)[3] are ancient microbial pattern recognition receptors highly conserved from *Drosophila* to humans. TLRs play a central role in the activation of the innate immune response and the pathogen recognition molecules that have important roles in detecting microbes and initiating inflammatory responses (4). The intracellular signaling pathways activated by the TLRs are mediated through the Toll/interleukin 1 (IL-1) receptor homology domains. Activation of signaling through the Toll/IL-1 receptor homology domains results in recruitment of the adaptor protein MyD88 and ultimately leads to degradation of IκB and translocation of NF-κB to the nucleus (4). Lipopolysaccharide (LPS), a component of the outer membrane of Gram-negative bacteria, is one of the most powerful activators of the TLR4 signaling. LPS is also well

* This work was supported by research grants from the Ministry of Education, Culture, Sports, Science, and Technology in Japan (to T. S. and K. U.).
[S] This article contains supplemental spectral data of isothiocyanate derivatives, Figs. S1–S6, and Table S1.
[1] These authors contributed equally to this work.
[2] To whom correspondence should be addressed: Laboratory of Food and Biodynamics, Graduate School of Bioagricultural Sciences, Nagoya University, Nagoya 464-8601, Japan. Tel.: 81-52-789-4127; Fax: 81-52-789-5296; E-mail: uchidak@agr.nagoya-u.ac.jp.

[3] The abbreviations used are: TLR, Toll-like receptor; IRAK4, interleukin 1 receptor-associated kinase 4; UPLC, ultraperformance LC; ESI, electrospray ionization; F, forward; R, reverse; Q4′G, quercetin 4′-*O*-β-glucoside; Al, alkynylated.

known to induce the production of proinflammatory mediators, such as tumor necrosis factor α (TNF-α), the β form of pro-IL-1, IL-6, and NO, and the activation of the MAPK signaling pathway and NF-κB, leading to death from endotoxin shock in animal models (5–7). In addition to TLR4, TLR2 has been shown to play a key role in the microbial component-induced activation of NF-κB (8). TLR2 recognizes lipoproteins that are anchored to the bacterial membrane by lipid chains covalently attached to the conserved N-terminal cysteine (9). The ligand binding specificity of TLR2 is modulated by its heterodimerization partners. TLR2 has been shown to be activated by many microbial products in addition to lipoproteins, including lipoteichoic acids, lipomannans, peptidoglycans, and zymosans (10).

Diets rich in vegetables are associated with the reduced risk of several major diseases, including atherosclerosis and other related inflammatory disorders (11, 12). Although some beneficial phytochemicals might function solely as antioxidants, it is becoming clear that many of the chemicals in vegetables and fruits evolved as toxins that exert beneficial anti-inflammatory effects in a variety of cells. In addition, based on the fact that the deregulation of the TLR activity is closely linked to the risk of inflammatory and immune disorders (13), TLRs and downstream signaling molecules can be the targets of many phytochemicals. In the present study, using reporter assay systems that potently respond to the TLR ligands, we determined the TLR signaling inhibitory potencies of food plants and found that cabbage and onion extracts most potently inhibited the TLR signaling. We performed an analysis of the cabbage and onion extracts and identified isothiocyanate and flavonoid compounds as the principal inhibitors of the TLR signaling. Moreover, we investigated the TLR inhibition potency of the compounds *in vitro* and propose a possible functional mechanism.

EXPERIMENTAL PROCEDURES

Materials—Goat anti-TLR4 (L-14) polyclonal antibody, rabbit anti-HA-probe (Y-11) polyclonal antibody, rabbit anti-MyD88 (HFL-296), goat anti-COX-2 (M-19) polyclonal antibody, goat anti-NOS2 (M-19) polyclonal antibody, goat anti-NF-κB (C-20) polyclonal antibody, and anti-IκB (C-21) polyclonal antibody were obtained from Santa Cruz Biotechnology. Anti-rabbit IgG, anti-mouse IgG-conjugated horseradish peroxidase, enhanced chemiluminescence (ECL) Western blotting detection reagents, and PVDF membranes were obtained from GE Healthcare. Anti-goat IgG-conjugated horseradish peroxidase was from Dako. The antibodies against ERK, phospho-ERK, JNK, phospho-JNK, p38, phospho-p38, interleukin 1 receptor-associated kinase 4 (IRAK4), phospho-IRAK4, phospho-TBK1, and TBK1 were obtained from Cell Signaling Technology. The anti-His tag polyclonal antibody was obtained from Medical and Biological Laboratories, Co., Ltd. (Nagoya, Japan). LPS and anti-lamin A antibody were purchased from Sigma. The protein concentration was measured using the BCA protein assay reagent obtained from Thermo. pUNO-HA-mouse TLR4, pUNO-HA-mouse TLR3, pUNO-HA-mouse-TLR6, Pam_2CSK_4, Pam_3CSK_4, polyinosinic-polycytidylic acid (poly(I:C)), and anti-TLR2 neutralizing antibody were obtained from Invivogen. The pMetluc2-NF-κB reporter vector was obtained from Clontech. pCMV2-FLAG-mouse MyD88 was obtained from Addgene. pEFBOS-FLAGHis-mouse TLR4, pEFBOS-FLAGHis-mouse TLR2, and pEFBOS-FLAGHis-mouse MD2 were kind gifts from Dr. K. Miyake (University of Tokyo). The botanical nomenclature of the vegetable species investigated in this study is shown in supplemental Table S1.

Cell Culture and Stable Transfection of HEK293—The human embryonic kidney (HEK) 293 cells were maintained in Dulbecco's modified Eagle's medium (DMEM) (Nissui, Japan) supplemented with 10% fetal bovine serum (FBS), 100 units/ml penicillin, 100 μg/ml streptomycin, 588 μg/ml L-glutamine, and 0.16% $NaHCO_3$. The cells were incubated under a humidified atmosphere of 95% O_2 and 5% CO_2 at 37 °C. The HEK293 were transfected with vectors using Lipofectamine 2000 transfection reagent (Invitrogen). Thereafter, stable transfectants were isolated by selection on 500 μg/ml G418 for about 3 weeks. Single clones of the stably transfected cells were isolated by limiting dilution. Several G418-resistant stable clones were maintained in medium containing 500 μg/ml G418. The expressions of TLR2, TLR4, and MD2 were confirmed using reverse transcription-polymerase chain reaction (RT-PCR) (data not shown). All the experiments were performed under 10% FBS-containing DMEM.

Cell Culture and Stable Transfection of RAW264.7—The murine macrophage cell line RAW264.7 was maintained in Dulbecco's modified Eagle's medium supplemented with 10% FBS, 100 units/ml penicillin, 100 μg/ml streptomycin, 588 μg/ml L-glutamine, and 0.16% $NaHCO_3$. The cells were incubated under a humidified atmosphere of 95% O_2 and 5% CO_2 at 37 °C. The RAW264.7 cells were transfected with the pMetluc2-NF-κB reporter vector using Lipofectamine 2000 transfection reagent. Thereafter, stable transfectants were isolated by selection on 500 μg/ml G418 for about 3 weeks. Single clones of the stably transfected cells were isolated by limiting dilution. Several G418-resistant stable clones were maintained in medium containing 500 μg/ml G418. All the experiments were performed under 10% FBS-containing DMEM.

Luciferase Assay for the HEK293 and RAW264.7 Cells—The luciferase assay for NF-κB in the HEK293 and RAW264.7 cells was performed according to the manufacturer's instructions using the Ready-To-Glow secreted luciferase reporter assay kit (Clontech). Briefly, the cell culture in each well was transferred to the corresponding well on a 96-well assay plate, then the Ready-To-Glow secreted luciferase substrate was added, and the luciferase activity was measured as the emission at 450 nm using a 2030 multilabel plate reader (ARVO X3, PerkinElmer Life Sciences).

Extraction and Isolation from Cabbage—Boiled cabbages were smashed with a grater, and the homogenates were washed with hexane and then sequentially extracted with ethyl acetate. The resulting ethyl acetate extract was separated by reverse-phase HPLC (Jasco) on a Sunniest octadecylsilane column (4.6 × 250 mm; ChromaNik) eluted with a linear gradient of water containing 0.1% trifluoroacetic acid (solvent A) and acetonitrile containing 0.1% trifluoroacetic acid (solvent B) (time = 0 min, 5% B; 40 min, 100% B; 50 min, 100% B; 51 min, 5% B) at a flow rate of 0.8 ml/min, and the 16–20-min fractions,

which showed the most potent activity, were further analyzed/purified by reverse-phase HPLC under the following conditions: a Sunniest octadecylsilane column (4.6 × 250 mm) using a linear gradient of water containing 0.1% trifluoroacetic acid (solvent A) and acetonitrile containing 0.1% trifluoroacetic acid (solvent B) (time = 0 min, 10% B; 30 min, 20% B; 40 min, 100% B) at a flow rate of 0.8 ml/min. The purified compound was analyzed by UPLC-ESI-MS/MS (UPLC-TQD, Waters), FTIR (FT/IR 4000, Jasco), high resolution MS (Mariner ESI-TOF, ABI), and NMR (ARX 400, Bruker).

LC-MS/MS Analysis of Iberin—Mass spectrometric analyses were performed using an ACQUITY Xevo TQD system (Waters) equipped with an ESI probe and interfaced with a UPLC system (Waters). The sample injection volumes of 10 μl each were separated on a Waters ethylene bridged hybrid C_{18} 1.7-μm column (100 × 2.1 mm) at a flow rate of 0.3 ml/min. A discontinuous gradient of solvent A (H_2O containing 0.1% formic acid) and solvent B (acetonitrile containing 0.1% formic acid) was used as follows: 5% B at 0 min, 5% B at 1 min, 95% B at 8 min, 95% B at 9 min. Mass spectrometric analyses were performed on line using ESI-MS/MS in the positive ion mode with multiple reaction monitoring mode (cone potential, 20 eV; collision energy, 20 eV). The multiple reaction monitoring transition monitored was as follows: m/z 164.1 → 77.0.

Extraction and Isolation from Onion—The boiled onions were smashed with a grater, and the homogenates were washed with hexane and then sequentially extracted with ethyl acetate. The resulting ethyl acetate extract was separated by reverse-phase HPLC (Jasco) on a Sunniest *octadecylsilane* column (10 × 250 mm) eluted with a linear gradient of water containing 0.1% trifluoroacetic acid (solvent A) and acetonitrile containing 0.1% trifluoroacetic acid (solvent B) (time = 0 min, 5% B; 30 min, 50% B; 40–50 min, 100% B; 51 min, 5% B) at a flow rate of 2.5 ml/min, and fractions G and I, which showed the most potent activity, were further analyzed/purified by reverse-phase HPLC under the following conditions. For fraction G, a Sunniest phenylethyl column (10 × 250 mm; ChromaNik) and a linear gradient of water containing 0.1% trifluoroacetic acid (solvent A) and acetonitrile containing 0.1% trifluoroacetic acid (solvent B) (time = 0 min, 35% B; 30 min, 45% B; 31–40 min, 100% B; 45 min, 35% B) at a flow rate of 2.5 ml/min were used. For fraction I, a Sunniest *octadecylsilane* column (10 × 250 mm) under an isocratic condition of acetonitrile/water (50:50, v/v) in 0.1% trifluoroacetic acid at a flow rate of 2.5 ml/min was used. The purified compounds G and I were analyzed by UPLC-ESI-MS (UPLC-SQD, Waters) and NMR (ARX 400, Bruker).

Immunoblot Analysis—Cells were washed twice with phosphate-buffered saline, pH 7.2 and lysed with lysis buffer (50 mM Tris-HCl, pH 7.5, 150 mM NaCl, 1% Triton X-100, 0.5% sodium deoxycholate, 0.1% SDS, protease inhibitor mixture, and phosphatase inhibitor mixtures (Sigma)). After protein quantification, equal amounts of protein (total protein, 20–50 μg) were boiled with Laemmli sample buffer for 5 min at 80 °C. The samples were run on 10% SDS-polyacrylamide gels, transferred to a nitrocellulose membrane, incubated with 0.25% polyvinylpyrrolidone (Sigma) in TBS/T (Tris-buffered saline containing 10% Tween 20) for blocking, washed, and treated with the primary antibodies. After washing with TBS/T, the blots were further incubated for 1 h at room temperature with the anti-IgG antibody coupled to horseradish peroxidase in TBS/T. The blots were then washed three times in TBS/T before visualization. An ECL Prime kit was used for detection.

RNA Isolation and RT-PCR—The total RNA was isolated with TRIzol reagent (Invitrogen). The RNA concentration was determined by measuring the absorbance at 260 nm. The RT reaction was performed with 5 μg of total RNA and an oligo(dT) primer using a first-strand cDNA synthesis kit. The PCRs were carried out using 0.5 μl of cDNA in 25 μl of 10 mM Tris-HCl, pH 8.3 containing 50 mM KCl, 0.1% Triton X-100, 200 μM dNTPs, 1 μM forward primer, 1 μM reverse primer, and 2 units of rTaq DNA polymerase (Toyobo Co., Osaka, Japan). The following primers were used: TLR2, 5′-TTG CTC CTG CGA ACT CCT AT-3′ (F) and 5′-GCT TTC TTG GGC TTC CTC TT-3′ (R); TLR4, 5′-GGT GGC TGT GGA GAC AAA AT-3′ (F) and 5′-TCA ACC GAT GGA CGT GTA AA-3′ (R); MD2, 5′-CTC TTT TCG ACG CTG CTT TC-3′ (F) and 5′-CCA TGG CAC AGA ACT TCC TT-3′ (R); TNFα, 5′-CAG CCT CTT CTC ATT CCT GCT TGT G-3′ (F) and 5′-CTG GAA GAC TCC TCC CAG GTA TAT-3′ (R); MIP-2, 5′-GCC AGT GAA CTG CGC TGT CAA TGC-3′ (F) and 5′-GTT AGC CTT GCC TTT GTT CAG TAT C-3′ (R); IL-1α, 5′-ACA CTA TCT CAG CAC CAC TTG G-3′ (F) and 5′-GCA CCC GAC TTT GTTC TT TGG-3′ (R).

Measurement of NO Concentration—The concentration of NO in the culture supernatant was determined as nitrite using Griess reagent (1% sulfanilamide and 0.1% naphthylethylenediamine dihydrochloride in 2.5% H_3PO_4 (Sigma). RAW264.7 cells were seeded in a 96-well plate at 1×10^4 cells/well in 200 μl of complete medium/well and incubated for 24 h at 37 °C. The cells were pretreated with iberin for 30 min and then stimulated with LPS (100 ng/ml) for 24 h. Next, the supernatant of the cell culture medium was collected and assayed for NO production using Griess reagent. The culture medium (100 μl) was incubated with 100 μl of Griess reagent. The absorbance of the mixture was then measured at 550 nm using a microplate reader. The concentration of nitrite was converted into sodium nitrite concentration, which was used as the standard.

LPS Binding Assay—The RAW264.7 cells were plated at subconfluence in 96-well plates. Various concentrations of iberin or polymyxin B (Invivogen) were added for 30 min, and then biotinylated LPS (Invivogen) was added for 15 min in 10% FBS-containing DMEM. To terminate the experiment, the medium was quickly removed, and the cells were washed with cold PBS. The cells were incubated with 1% Block Ace (Yukijirushi) in PBS for 1 h at 37 °C. After washing the cells three times with PBS, HRP-conjugated avidin in PBS was added and then incubated for 1 h at 37 °C. After washing, 100 μl of 0.05 M citrate buffer, pH 5.0 containing 0.4 mg/ml *o*-phenylenediamine and 0.003% H_2O_2 was added and incubated for several minutes at room temperature in the dark. The reaction was terminated by the addition of 2 N sulfuric acid, and the absorbance at 492 nm was read using a microplate reader.

Immunoprecipitation for Detection of TLR Dimer—Protein extracts were prepared from HEK293 cells transiently expressing TLR4-His, MyD88-FLAG, and MD2 (for detection of TLR4-MyD88 complex); TLR2-His and TLR6-HA (for detec-

tion of TLR2-TLR6); or TLR4-His, TLR4-HA, and MD2 (for detection of TLR4 dimer). The lysate was incubated with the anti-His tag antibody for 12 h and further incubated with 70 μl of Dynabeads® Protein G (Invitrogen) for 6 h at 4 °C with rocking. The immune complexes were solubilized with Laemmli sample buffer after four washes with lysis buffer. The solubilized immune complex was resolved by SDS-PAGE, and immunoblot analysis was performed with anti-FLAG (for TLR4-MyD88 complex) or anti-HA (for TLR4 dimer or TLR2-TLR6 complex) antibody.

Click Chemistry—HEK293 cells transiently expressing His- or HA-tagged TLRs were treated with the alkynylated (Al) iberin analogues dissolved in methanol or the vehicle control (methanol only) for 1 h at 37 °C. The cells were then washed twice with cold PBS, lysed in radioimmune precipitation assay buffer (50 mM Tris-HCl, pH 7.5, 150 mM NaCl, 1% Nonidet P-40, 0.5% sodium deoxycholate, 0.1% SDS, protease inhibitor mixture, and phosphatase inhibitor mixtures 1 and 2), and centrifuged at 10,000 rpm for 10 min at 4 °C. Click chemistry was performed with cellular lysates containing 2.0 mg/ml protein with 1 mM $CuSO_4$, 1 mM ascorbic acid, 0.1 mM tris((1-benzyl-1*H*-1,2,3-triazol-4-yl)methyl)amine (Anaspec Inc., San Jose, CA), and 20 μM azide-PEG4-biotin conjugate (Click Chemistry Tools). After incubation in the dark for 1 h at room temperature, the cell lysate proteins were diluted with loading buffer and separated on an SDS-polyacrylamide gel, or the avidin pulldown was performed.

Avidin Pulldown Assay—UltraLink immobilized NeutrAvidin beads (Thermo) were added to the cell lysate, and the samples were rotated at 4 °C for 2 h to preclear the nonspecific binding to the NeutrAvidin beads. Next, click chemistry was performed with the supernatant in the dark for 2 h at room temperature. After incubation, the lysate containing the biotin-N_3 conjugation to the Al-isothiocyanate-modified proteins was incubated with NeutrAvidin beads for 4 h at 4 °C. The beads were then washed three times in radioimmune precipitation assay buffer, and the bound proteins were eluted into SDS sample buffer by boiling for 5 min. The biotinylated proteins were resolved by SDS-PAGE and subjected to immunoblot analysis with the anti-His or -HA tag antibody.

Synthesis of the Isothiocyanate Derivatives—Synthesis of the isothiocyanate derivatives for click chemistry is shown in supplemental Fig. S1. Chemoselective protection of the amino group of 3-aminopropanol with the *t*-butoxycarbonyl group followed by *O*-tosylation provided the tosylate. Conversion of the tosylate to thioester was achieved by treatment with potassium thioacetate. The thioacetate was converted to 3-butynylsulfide. Treatment with thiophosgene after removal of the *t*-butoxycarbonyl group provided the isothiocyanate followed by oxidation of the sulfide with 2-iodoxybenzoic acid resin to provide the sulfoxide. The isothiocyanate derivatives for the structure-activity relationship study were also synthesized by similar procedures. The spectral data of these compounds are described in the supplemental material.

Modeling Analysis—The structures were subsequently optimized using the Merck force field (MMFF94; Ref. 14) and the Born continuum solvation model (14, 15) as implemented in Molecular Operating Environment (MOE).

Animal Experiments—Eight-week-old female BALB/c mice (purchased from the Japan SLC, Hamamatsu, Japan) were orally administered with vehicle (corn oil) or iberin (50 mg/kg of body weight) at 1 h before intraperitoneal injection of LPS (5 mg/kg of body weight). Blood was collected at 4 h after LPS injection and allowed to clot at room temperature. Serum was separated by centrifugation and stored at −80 °C until analysis. Concentrations of the cytokine TNF-α were determined using the Quantikine ELISA kit specific for each cytokine according to the manufacturer's instructions (R&D Systems). All animal protocols were approved by the Animal Experiment Committee in the Graduate School of Bioagricultural Sciences, Nagoya University.

RESULTS

Inhibition of TLR Signaling by Vegetable Extracts—To investigate the anti-inflammatory potential of the phytochemicals contained in vegetables, we first attempted to develop a luciferase reporter assay system that detects the TLR-dependent activation of NF-κB. To this end, we established TLR4- and TLR2-expressing cells (HEK293-TLR4/MD2 and HEK293-TLR2 cells) by stable transfection with TLR4/MD2 and TLR2, respectively (Fig. 1). Using these assay systems, we screened a number of vegetable extracts for the inhibition of the ligand-dependent TLR activation and found that the cabbage, onion, and beet extracts showed a remarkable inhibition of both the TLR4- and TLR2-dependent signaling (Fig. 2, *A* and *B*). Among them, we focused on the cabbage and onion extracts because of their high consumption and prevalence. Dose-dependent inhibitions of both the LPS-dependent activation of TLR4 and Pam_3CSK_4-dependent activation of TLR2 by the cabbage extracts are shown in Fig. 2, *C* and *D*, respectively. Similar results were also obtained with the onion extracts (data not shown).

Identification of Dietary TLR Signaling Inhibitors—To identify the active component responsible for the inhibition of the TLR signaling, we performed the activity-guiding separation of a principal inducer from the cabbage and onion. The cabbages were extracted with ethyl acetate, and the extract was fractionated into 15 fractions by reverse-phase HPLC (Fig. 3*A*). As shown in Fig. 3*B*, the 16–20-min fraction exhibited the most potent inhibitory activity. We further separated this fraction by HPLC, and we detected 14 chromatographic peaks (Fig. 3*C*) and found that peak 6 had a significant inhibitory activity toward the ligand-induced TLR4 activities (Fig. 3*D*). The spectroscopic data, including ^1H and ^{13}C NMR, FTIR, MS/MS fragmentation, and high resolution MS (molecular ion at *m*/*z* 164.01983, $[M + H]^+$, $C_5H_{10}NOS_2$), of this compound were completely identical to those of 3-methylsulfinylpropyl isothiocyanate (iberin) (Fig. 3, *E*–*G*, and supplemental Figs. S2 and S3). The ligand-induced TLR signaling was significantly inhibited in the low micromolar range by iberin (Fig. 4, *A* and *B*). Iberin was detected in cabbage and red cabbage but not in watercress, broccoli, and Chinese cabbage, and the amount of iberin contained in the cabbage extract was ~8.6 nmol/mg of extract, which accounts for ~80% of the total inhibitory activity of the cabbage extract (Fig. 4, *C* and *D*).

Iberin also showed an anti-inflammatory effect on the macrophages activated by the TLR ligands *in vitro* (Fig. 5, *A*–*E*)

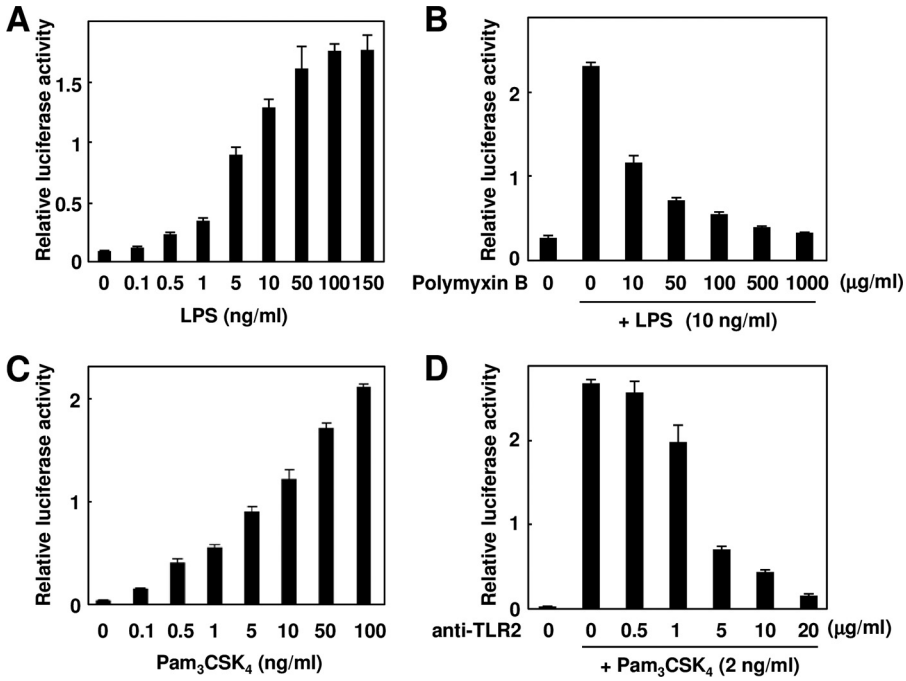

FIGURE 1. **Development of TLR-expressing derivatives of HEK293 cells (HEK293-TLR4/MD2 and HEK293-TLR2 cells) by stable transfection.** *A*, LPS-dependent induction of luciferase activity. The HEK293-TLR4/MD2 cells were treated with each concentration of LPS (0–150 ng/ml) for 24 h. The results shown are means ± S.D. (*error bars*) of three independent experiments. *B*, effect of polymyxin B on LPS-induced luciferase activity. The HEK293-TLR4/MD2 cells were pretreated with each concentration of polymyxin B (0–1000 μg/ml) and then treated with 10 ng/ml LPS for 24 h. The results shown are means ± SD (*error bars*) of three independent experiments. *C*, Pam_3CSK_4-dependent induction of luciferase activity. The HEK293-TLR2 cells were treated with each concentration of Pam_3CSK_4 (0–100 ng/ml) for 24 h. The results shown are means ± S.D. (*error bars*) of three independent experiments. *D*, effect of anti-TLR2 neutralizing antibody on Pam_3CSK_4-induced luciferase activity. The HEK293-TLR2 cells were pretreated with each concentration of anti-TLR2 neutralizing antibody (0–20 μg/ml) and then treated with 2 ng/ml Pam_3CSK_4 for 24 h. The results shown are means ± S.D. (*error bars*) of three independent experiments.

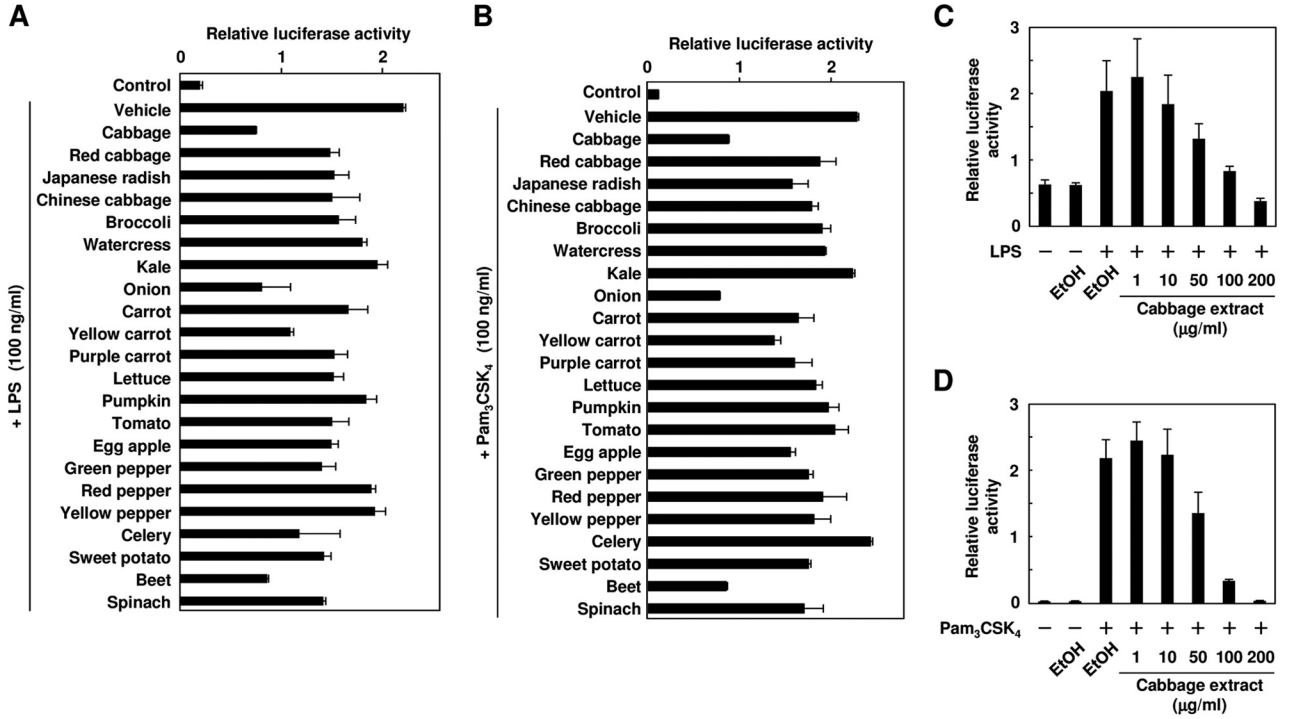

FIGURE 2. **TLR inhibitor potency of extracts from vegetables.** *A* and *B*, the HEK293-TLR4/MD2 cells (*A*) or HEK293-TLR2 cells (*B*) were pretreated with 100 μg/ml ethyl acetate extracts for 30 min and then treated with 100 ng/ml LPS (*A*) or Pam_3CSK_4 (*B*) for 24 h. The results shown are means ± S.D. (*error bars*) of three independent experiments. *C* and *D*, the HEK293-TLR4/MD2 cells (*C*) or the HEK293-TLR2 cells (*D*) were pretreated with each concentration of the ethyl acetate extracts from cabbage for 30 min and then treated with 100 ng/ml LPS (*C*) or Pam_3CSK_4 (*D*) for 24 h. The results shown are means ± S.D. (*error bars*) of three independent experiments.

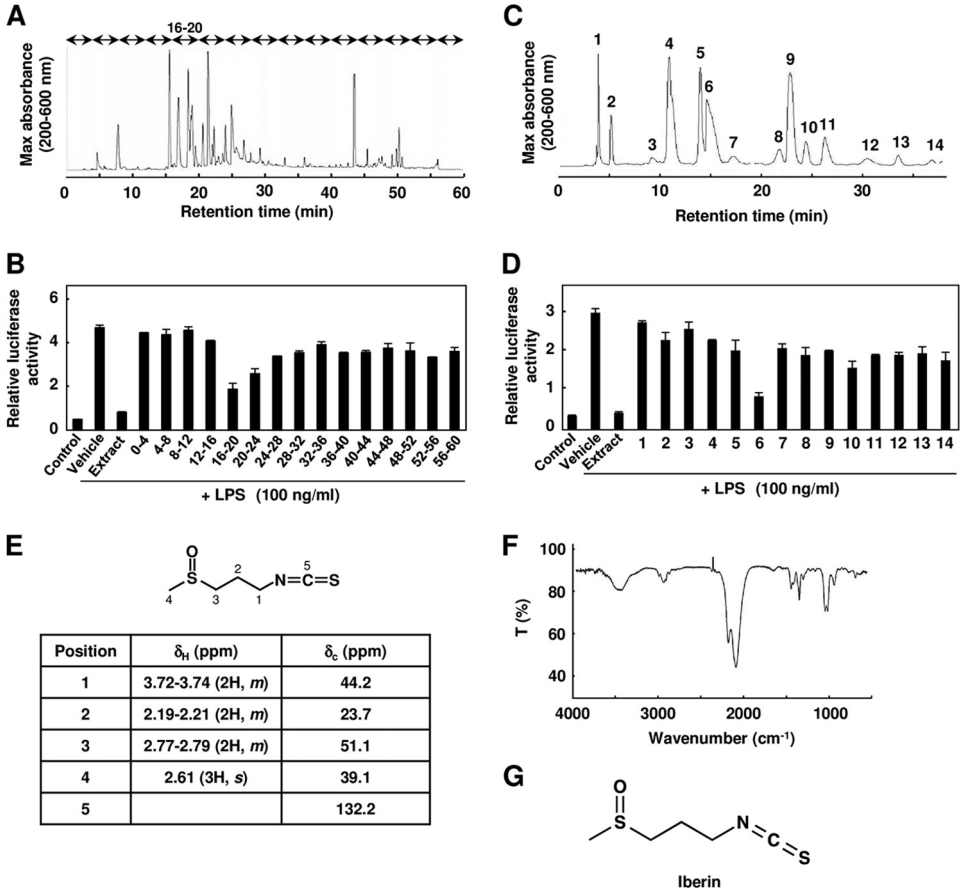

Position	δ_H (ppm)	δ_c (ppm)
1	3.72-3.74 (2H, *m*)	44.2
2	2.19-2.21 (2H, *m*)	23.7
3	2.77-2.79 (2H, *m*)	51.1
4	2.61 (3H, *s*)	39.1
5		132.2

FIGURE 3. **Identification of TLR inhibitor from cabbage.** *A*, the ethyl acetate extract from cabbage was analyzed by reverse-phase HPLC. *B*, TLR4 inhibitor potency of fractions separated by reverse-phase HPLC. The ethyl acetate extract of cabbage was fractionated every 4 min and divided into 15 factions by HPLC. The HEK293-TLR4/MD2 cells were pretreated with each fraction and then treated with 100 ng/ml LPS for 24 h. The results shown are means ± S.D. (*error bars*) of three independent experiments. *C*, the 16–20-min fraction in *A* was analyzed by reverse-phase HPLC. *D*, TLR4 inhibitor potency of the peaks separated by reverse-phase HPLC. The cells were pretreated with each peak and then treated with 100 ng/ml LPS for 24 h. The results shown are means ± S.D. (*error bars*) of three independent experiments. *E*, the ^{1}H and ^{13}C NMR analysis of iberin isolated from cabbage extract. *F*, FTIR spectrum of the iberin isolated from cabbage extract: 1017 and 1047 cm^{-1}, ν(S=O); 1348 and 1443 cm^{-1}, δ(C–H) from CH_3 and CH_2; 2091 and 2180 cm^{-1}, ν(-N=C=S); 2934 cm^{-1}, ν(C–H) from CH_3 and CH_2 IR (liquid film, $CHCl_3$); ν_{max}, 3002 (CH stretch), 2108 (-N=C=S), and 1032 cm^{-1} (sulfinyl). *G*, chemical structure of iberin.

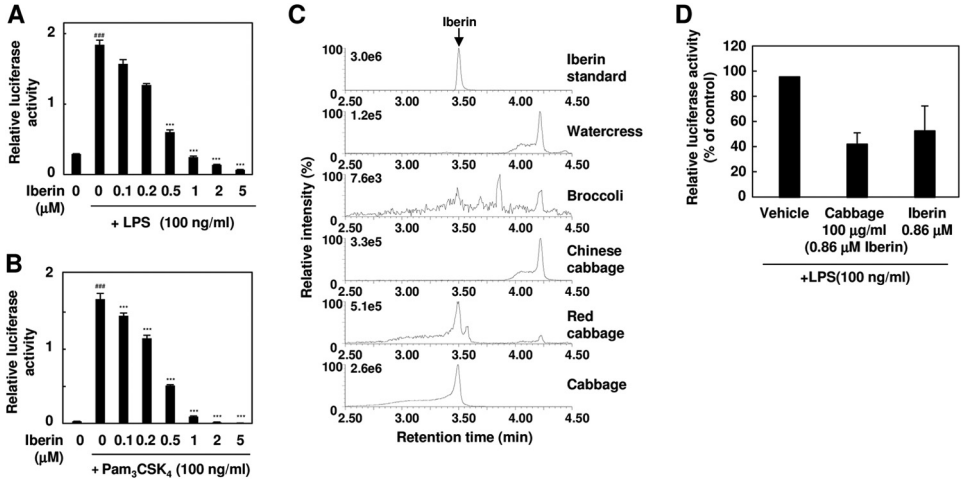

FIGURE 4. **Iberin is a major TLR inhibitor in cabbage extract.** *A* and *B*, TLR4 and TLR2 inhibitor potency of iberin. The HEK293-TLR4/MD2 cells (*A*) or HEK293-TLR2 cells (*B*) were pretreated with iberin for 30 min and then treated with 100 ng/ml LPS (*A*) or Pam_3CSK_4 (*B*) for 24 h. The results shown are means ± S.D. (*error bars*) of three independent experiments. ###, $p < 0.005$ *versus* control; ***, $p < 0.005$ *versus* ligand alone. *C*, LC-ESI-MS/MS analysis of iberin in vegetable extracts. The ion current tracing of iberin using LC-ESI-MS/MS with multiple reaction monitoring is shown. *D*, the comparison of cabbage extract and purified iberin on TLR4 inhibition. The HEK293-TLR4/MD2 cells were pretreated with vehicle (ethanol), cabbage extract (100 μg/ml; containing ~0.86 μM iberin), or purified iberin (0.86 μM) for 30 min and then treated with 100 ng/ml LPS. *Error bars* represent S.D.

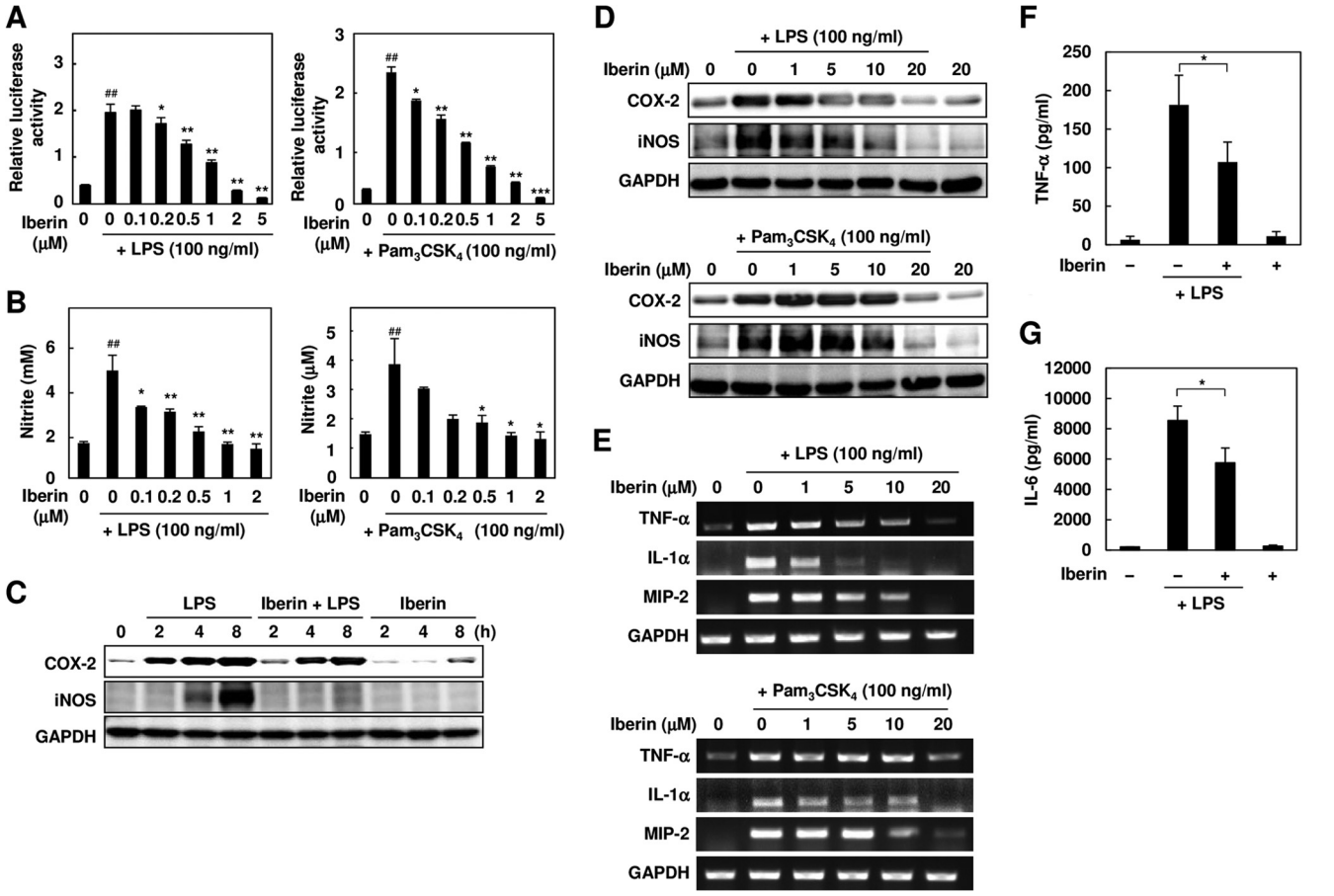

FIGURE 5. **Anti-inflammatory effects of iberin *in vitro* and *in vivo*.** *A*, the RAW264.7 cells expressing the NF-κB reporter gene were pretreated with iberin (0–5 μM) for 30 min and then treated with 100 ng/ml LPS (*left panel*) or Pam_3CSK_4 (*right panel*) for 24 h. ##, $p < 0.01$ *versus* control; *, $p < 0.05$ and **, $p < 0.01$ *versus* ligand alone. 0 μM iberin denotes vehicle without iberin. *Error bars* represent S.D. *B*, analysis of NO production. The RAW264.7 cells were pretreated with iberin (0–2 μM) for 30 min and then treated with 100 ng/ml LPS (*left panel*) or Pam_3CSK_4 (*right panel*) for 24 h. After treatment, the NO production was analyzed using the Griess method. ##, $p < 0.01$ *versus* control; *, $p < 0.05$; **, $p < 0.01$, and ***, $p < 0.005$ *versus* ligand alone. 0 μM iberin denotes vehicle without iberin. *Error bars* represent S.D. *C*, the RAW264.7 cells were pretreated with iberin (10 μM) for 30 min and then treated with 100 ng/ml LPS for the indicated times (2, 4, and 8 h). After treatment, inflammation-related gene expression was analyzed by immunoblot analysis. *D*, the RAW264.7 cells were pretreated with iberin (0–20 μM) for 30 min and then treated with 100 ng/ml LPS (*top*) or Pam_3CSK_4 (*bottom*) for 24 h. After treatment, inflammation-related gene expression was analyzed by immunoblot analysis. *E*, the RAW264.7 cells were pretreated with iberin (0–20 μM) for 30 min and then treated with 100 ng/ml LPS (*top*) or Pam_3CSK_4 (*bottom*) for 8 h. After treatment, inflammation-related gene expression was analyzed by RT-PCR analysis. *F* and *G*, iberin inhibits LPS-induced production of inflammatory cytokines in mice. Iberin (50 mg/kg of body weight) was orally administered 1 h before LPS challenge (5 mg/kg of body weight; intraperitoneal) in mice. Serum samples were collected 4 h after LPS challenge. Serum concentrations of TNF-α (*F*) and IL-6 (*G*) were determined by specific ELISA. Values are mean ± S.D. (*error bars*) ($n = 4$). Corn oil was used as the vehicle (*Veh*). *, $p < 0.05$.

and on the LPS-induced inflammation *in vivo* (Fig. 5, *F* and *G*). However, iberin did not inhibit the NF-κB activity induced by phorbol 12-myristate 13-acetate, a TLR-independent proinflammatory ligand (data not shown). These data strongly suggest that iberin specifically acts on the TLR-dependent signaling.

To identify the active components in onion, the ethyl acetate extracts of the onion were fractionated into 11 fractions (fractions A–K) by reverse-phase HPLC and subjected to the TLR signaling inhibitory assay (Fig. 6, *A* and *B*). We detected two major active fractions, G and I, which were further separated and purified by reverse-phase HPLC (Fig. 6, *C* and *D*). The purified compounds from fractions G and I showed significant TLR4 inhibitory potencies (Fig. 5, *E* and *F*) and were then submitted for structural characterization without further purification. The LC-ESI-MS spectrum of compound I showed a molecular ion, $[M - H]^-$, at m/z 301.1 (supplemental Fig. S4A). The ^1H and ^{13}C NMR spectra of compound I exhibited resonances due to aromatic systems (supplemental Fig. S5A). In the ^1H NMR spectrum of compound I, the aromatic region exhibited an ABX system at δ 7.82 (1H, d, $J = 2.9$ Hz, H-2′), 7.72 (1H, d, $J = 2.9$ Hz, H-6′), and 6.97 (1H, d, $J = 2.9$ Hz, H-5′) due to the 3′,4′ disubstitution of ring B and a typical meta-coupled pattern for the H-6 and H-8 protons (δ 6.27 and 6.47, d, $J = 2.0$ Hz). The ^{13}C NMR spectrum of compound I showed the presence of 15 aromatic carbon signals. Based on these NMR data and comparison with the data given in the literature, the structure of compound I was identified as quercetin (Fig. 7*A*). We also characterized compound G by LC-ESI-MS and NMR. The mass spectrum of compound G showed two major peaks at m/z 463.2 $[M - H]^-$ and 301.1 $[M - H - 162]^-$ (supplemental Fig. S4B), suggesting that it was composed of one molecule of aglycone and one monosaccharide molecule. The ^1H and ^{13}C NMR spectra indeed showed the presence of quercetin and a sugar moiety (supplemental Fig. S5B). In addition, all of the glycosidic protons were assigned by the ^1H NMR and the ^1H-^1H COSY. The

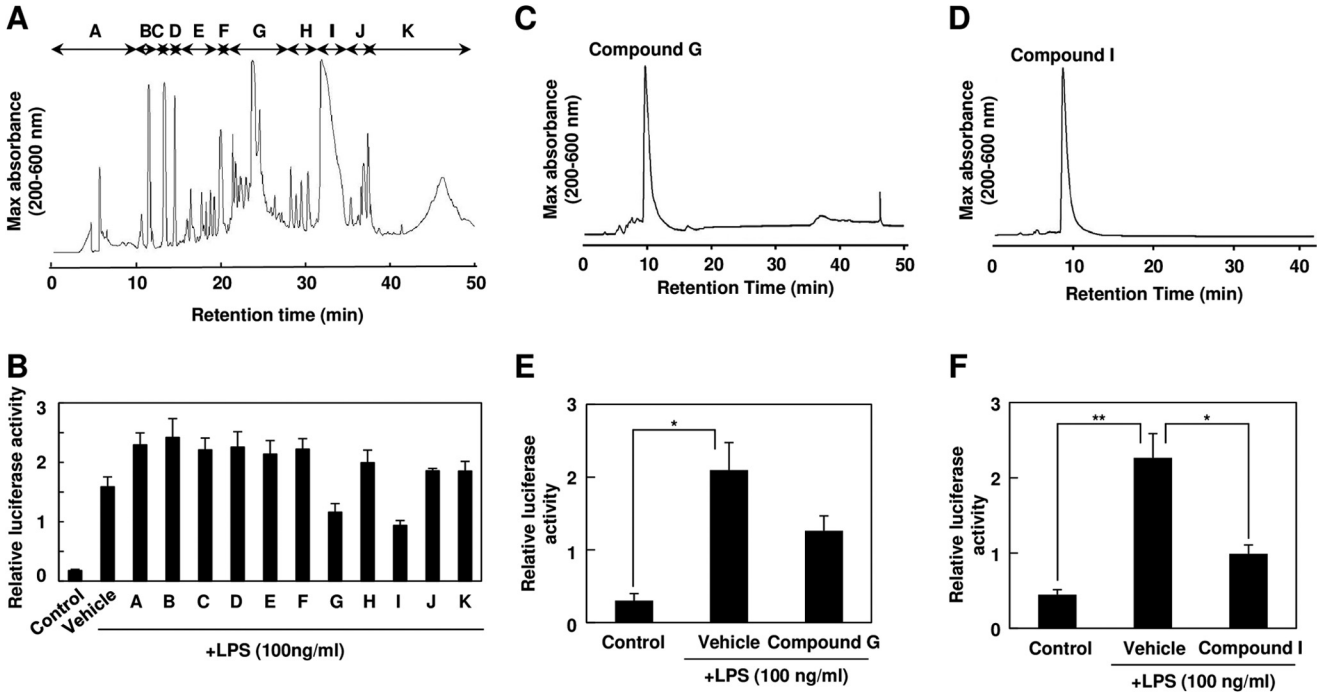

FIGURE 6. **Identification of TLR inhibitor from onion.** *A*, the ethyl acetate extract from onion was analyzed by reverse-phase HPLC. *B*, TLR4 inhibitor potency of the fractions separated by reverse-phase HPLC. The ethyl acetate extract of onion was fractionated into 11 fractions (fractions A–K) as shown in *A*. The cells were pretreated with each fraction and then treated with 100 ng/ml LPS for 24 h. The results shown are means ± S.D. (*error bars*) of three independent experiments. *C* and *D*, fraction G (*C*) and fraction I (*D*) in *A* were analyzed by reverse-phase HPLC under the conditions described under "Experimental Procedures." *E*, TLR4 inhibitor potency of compound G separated by reverse-phase HPLC as shown in *C*. The cells were pretreated with 500 μg/ml compound G for 30 min and then treated with 100 ng/ml LPS for 24 h. The results shown are means ± S.D. (*error bars*) of three independent experiments. *, $p < 0.05$. *F*, TLR4 inhibitor potency of compound I separated by reverse-phase HPLC as shown in *D*. The cells were pretreated with 500 μg/ml compound I for 30 min and then treated with 100 ng/ml LPS for 24 h. The results shown are means ± S.D. (*error bars*) of three independent experiments. *, $p < 0.05$; **, $p < 0.01$.

sugar region of the spectrum of compound G revealed one anomeric hydrogen signal at 5.00 ppm (H-1″, d, $J = 7.6$ Hz), suggesting the β-configuration for the sugar. Moreover, the resonances in the region of δ 3.30–3.80 (6H, m, H-2″, H-3″, H-4″, H-5″, H-6″) together with the corresponding carbon resonances inferred by the *heteronuclear multiple quantum correlation* spectrum suggested the presence of a β-glucopyranose unit. Furthermore, the cross-peak from the anomeric proton H-1″ (δ 5.00) of glucose to C-4′ (δ 1460.79) of quercetin in the *heteronuclear multiple bond correlation* spectrum indicated that the glucose was conjugated to the C-4′ position of quercetin (supplemental Fig. S6). Therefore, it was concluded that peak G was quercetin 4′-*O*-β-glucoside (Q4′G) (Fig. 7*B*). Quercetin and Q4′G showed dose-dependent inhibitions of the ligand-induced activation of TLR4 and TLR2 (Fig. 7, *C*–*F*). When cells were preincubated with 25 μM quercetin or Q4′G, the activities were reduced ~50%.

Inhibition of TLR Dimerization by Iberin—Because iberin showed the most potent TLR signaling inhibitory activity among the three inhibitors isolated from cabbage and onion, we characterized the molecular mechanism mainly focusing on iberin. To examine the effect of iberin on the ligand recognition by TLRs as the initial event, we first performed the biotin-LPS binding assay of RAW264.7 cells using cell-based ELISA with avidin-HRP conjugates and observed that iberin did not have any effect on the ligand binding of TLR4 (Fig. 8*A*). Thus, iberin is likely to act on the TLRs and/or their downstream signaling.

It has been established that activation of the TLRs results in the recruitment of the adaptor protein MyD88, which recruits IRAK4, a key mediator in the TLR/IL-1 receptor signaling pathway, and induces IRAK4 phosphorylation, which ultimately leads to degradation of IκB and translocation of NF-κB to the nucleus (Fig. 8*B*) (4). Indeed, the overexpression of TLR2 dramatically activated NF-κB, and iberin showed its inhibitory effect toward the TLR2 overexpression-induced activation of NF-κB (Fig. 8*C*). However, iberin only slightly (and not significantly) inhibited the MyD88-induced activation of NF-κB (Fig. 8*D*), suggesting that iberin exerts its inhibitory effect at a step that is upstream of MyD88. We also found that iberin did not inhibit poly(I:C)-induced (MyD88-independent) phosphorylation of TBK1 (Fig. 8*E*). In addition, iberin inhibited the LPS-stimulated formation of the TRL4-MyD88 complex (Fig. 8*F*) and phosphorylation of IRAK4 (Fig. 8*G*). These data suggest that iberin may act on TLRs as the target.

Receptor dimerization is one of the initial steps triggering the TLR signaling pathways (16). Hence, we investigated whether iberin affected the dimerization of TLRs by an immunoprecipitation experiment using HEK293 cells expressing both HA-tagged TLR4 and His-tagged TLR4. The HA-tagged TLR4 was co-precipitated with the His-tagged TLR4 upon LPS stimulation, indicating the association of the His-tagged TLR4 and the HA-tagged TLR4 to form dimers, and iberin attenuated the LPS-induced association between the HA-tagged TLR4 and the His-tagged TLR4 (Fig. 8*H*). In addition, the interaction of TLR2 and TLR6 was also disrupted by iberin (Fig. 8*I*).

The inhibition of TLR dimerization by iberin resulted in the attenuation of the downstream intracellular TLR signaling, such as the NF-κB and MAPK pathways (Fig. 9, *A*–*D*). There

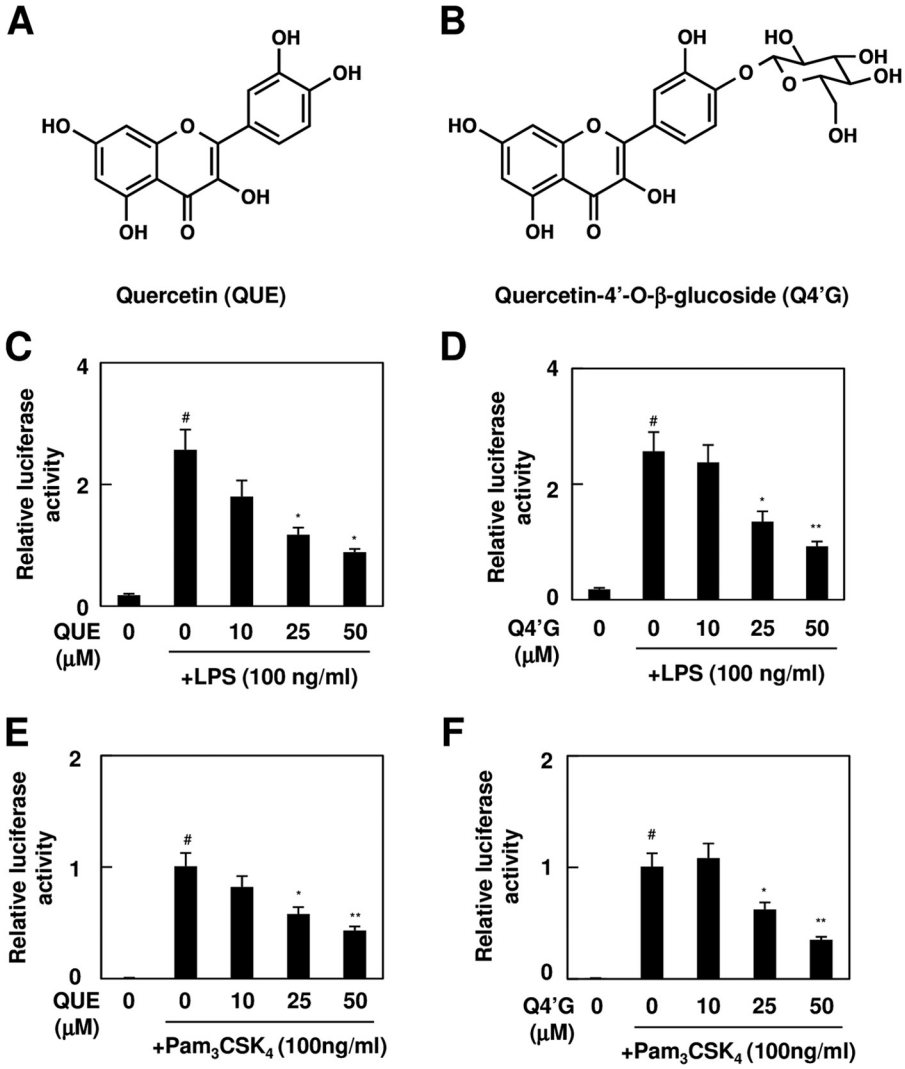

FIGURE 7. **TLR inhibitor potency of quercetin and quercetin 4′-*O*-β-glucoside.** *A* and *B*, chemical structure of quercetin (*A*) and Q4′G (*B*). *C–F*, TLR inhibitor potency of quercetin (*QUE*) and Q4′G. The HEK293-TLR4 cells (*C* and *D*) or HEK293-TLR2 cells (*E* and *F*) were pretreated with quercetin (*C* and *E*) or Q4′G (*D* and *F*) for 30 min and then treated with 100 ng/ml LPS (*C* and *D*) or Pam_3CSK_4 (*E* and *F*) for 24 h. The results shown are means ± S.D. (*error bars*) of three independent experiments. #, $p < 0.05$ *versus* control; *, $p < 0.05$ and **, $p < 0.01$ *versus* ligand alone.

exists a threshold (~5 μM iberin) above which an anti-inflammatory response is produced. Such a biphasic profile was previously shown for the mitogen-activated protein kinase inhibition in LPS-stimulated cells by TAK-242, a synthetic TLR4 inhibitor (17). We also tested the effect of quercetin and Q4′G on the dimerization of TLR4 but observed no significant effect (data not shown). However, both quercetin and Q4′G significantly suppressed the activation of NF-κB induced by the MyD88 overexpression (Fig. 9*E*). These and the observation that poly(I:C)-induced apoptosis signaling was not affected by quercetin and Q4′G (Fig. 9*F*) suggest that quercetin and Q4′G may act downstream of MyD88.

Covalent Modification of TLR4 by Iberin—Because isothiocyanate compounds, including iberin, specifically react with the thiol moiety in proteins, we examined the effects of the thiol compounds, including dithiothreitol (DTT) and *N*-acetylcysteine, on the inhibition of the TLR4 signaling by iberin. The pretreatments with DTT and *N*-acetylcysteine significantly suppressed the TLR4 inhibitory activity of iberin (Fig. 10, *A* and *B*), suggesting that the TLR4 inhibition by iberin was dependent on its reactivity to the thiol group. Similar results were obtained when the effect of the thiol compounds was examined for the inhibition of TLR2 signaling by iberin (Fig. 10, *C* and *D*). Based on these results and the fact that TLRs are type I transmembrane receptors consisting of a cysteine-rich region in the extracellular domain and Toll/IL-1 receptor homology region in the cytoplasmic domain, we hypothesized that the inhibition of the TLR4 signaling by iberin might be largely due to direct modification of TLR4 by iberin.

To investigate whether iberin could react with the cysteine residues in TLR4, a probe combining an isothiocyanate-reactive group and an alkyne functionality was designed. The presence of the alkyne functionality could then be detected in a later step upon the Cu(I)-catalyzed Huisgen [3 + 2] cycloaddition ("click chemistry") reaction (18) with an azide-functionalized biotin group. The alkynylated iberin analogues, such as Al-iberin and its analogue Al-iberverin (Fig. 11*A*), were synthesized (supplemental Fig. S1) and examined for modification of

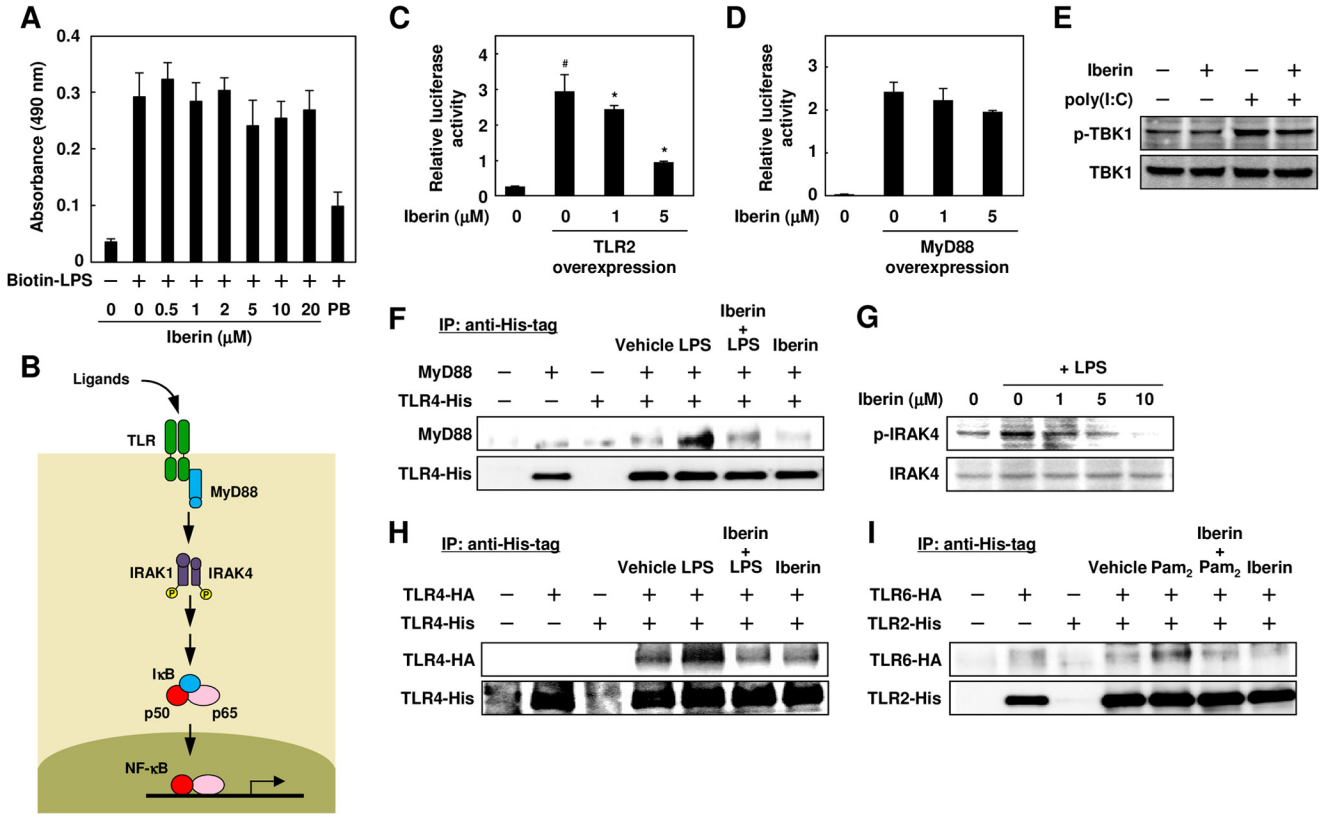

FIGURE 8. **Inhibition of TLR dimerization by iberin.** *A*, effect of iberin on the binding of LPS to RAW264.7 cells. The cells were pretreated with iberin (0–20 μM) or polymyxin B (*PB*; 100 μg/ml) for 30 min and then treated with 300 ng/ml biotin-labeled LPS (*Biotin-LPS*) for 15 min. After incubation, the cells were analyzed by ELISA using HRP-conjugated avidin. *Error bars* represent S.D. *B*, the TLR/NF-κB signaling pathway. *C*, effect of iberin on NF-κB activation mediated by TLR2. The HEK293 cells were transiently co-transfected with the expression plasmid for TLR2 or empty vector and NF-κB reporter plasmid. After transfection, the cells were cultured in the absence or presence of iberin for 24 h. #, $p < 0.05$ *versus* control; *, $p < 0.05$ *versus* TLR2 overexpression (0 μM iberin). *Error bars* represent S.D. *D*, effect of iberin on NF-κB activation mediated by MyD88. HEK293 cells were transiently co-transfected with the expression plasmid for adaptor protein MyD88 or empty vector and NF-κB reporter plasmid. After transfection, the cells were cultured in the absence or presence of iberin for 24 h. *Error bars* represent S.D. *E*, effect of iberin on poly(I:C)-induced phosphorylation of TBK1 (*p-TBK1*). RAW264.7 cells were pretreated with iberin (10 μM) for 30 min and then treated with poly(I:C) (10 μg/ml) for 30 min. *F*, effect of iberin on co-immunoprecipitation of MyD88 with TLR4. The HEK293 cells were transfected with expression vectors encoding TLR4-His and/or MyD88 together with MD2. Twenty-four hours after transfection, the cells were pretreated with iberin (15 μM) for 30 min and then treated with LPS (500 ng/ml) for 20 min. After incubation, the cells were washed and lysed. The cell lysates were immunoprecipitated (*IP*) with the anti-His-tag antibody, and the immunoprecipitates were analyzed by immunoblotting using the anti-MyD88 and anti-His tag antibodies. *G*, immunoblot analysis of phosphorylation of IRAK4. The RAW 264.7 cells were pretreated with iberin for 60 min and then treated with LPS (100 ng/ml) for 30 min. *H*, inhibition of TLR4 dimerization by iberin. The HEK293 cells expressing TLR4-HA and/or TLR4-His together with MD2 were pretreated with iberin (20 μM) for 30 min and then treated with LPS (500 ng/ml) for 20 min. The cells were then subjected to immunoprecipitation with anti-His tag antibody and immunoblotted with the anti-HA tag (*upper*) or anti-His tag (*lower*) antibody. *I*, inhibition of TLR2/TLR6 heterodimerization by iberin. The HEK293 cells expressing TLR2-His and/or TLR6-HA were pretreated with iberin (20 μM) for 30 min and then treated with Pam_2CSK_4 (500 ng/ml) for 20 min. The cells were then subjected to immunoprecipitation with the anti-His tag antibody and immunoblotted with anti-HA tag (*upper*) or anti-His tag (*lower*) antibody.

cellular proteins in the RAW264.7 cells. After exposure of the cells to these alkynylated iberin analogues, click chemistry was performed with cellular lysates followed by the separation of the lysate proteins by SDS-PAGE. In accordance with the reversible nature of the reactions, a dramatic increase in the protein-bound label was observed when the cells were incubated with Al-iberin, whereas only a slight labeling was observed in the Al-iberverin-treated cells (Fig. 11*B*). We then attempted to detect the iberin-TLR adduct in the cells exposed to Al-iberin. Hence, the binding of Al-iberin to the TLRs was confirmed by a pulldown assay. To this end, the TLR4-HA-, TLR3-HA-, or TLR2-His-transfected HEK293 cells were treated with 20 μM Al-iberin, and then biotin-N_3 conjugation to the Al-iberin-modified proteins from the cellular lysates was done using click chemistry. Pulldown with NeutrAvidin beads followed by Western blotting with an anti-HA or -His antibody consistently demonstrated the binding of the Al-iberin analogues to TLR4 and TLR2 but not to TLR3 (Fig. 11, *C* and *D*). The covalent binding of the iberin probe to TLR4 and TLR2 was also confirmed by immunoprecipitation analysis using the anti-HA and -His tag antibodies, respectively (Fig. 11, *E* and *F*). Thus, it was revealed that iberin could modify plasma membrane-associated TLRs, such as TLR2 and TLR4. These results suggest that iberin may inhibit the TLR dimerization via covalent binding to the receptor (Fig. 11*G*).

Structure-Activity Relationship of Isothiocyanates—A variety of isothiocyanate compounds are found in vegetables, especially cruciferous species, including cabbage. To define the structural features of iberin important for the inhibitory effects, we synthesized the analogues of iberin and measured their inhibitor potencies against the LPS-induced (Fig. 12*A*, *panels a*, *c*, and *e*) and Pam_3CSK_4-induced (*panels b*, *d*, and *f*) activation of the TLR signaling. As shown in Fig. 12*A*, the number of methylene groups in the bridge linking the isothiocyanate and

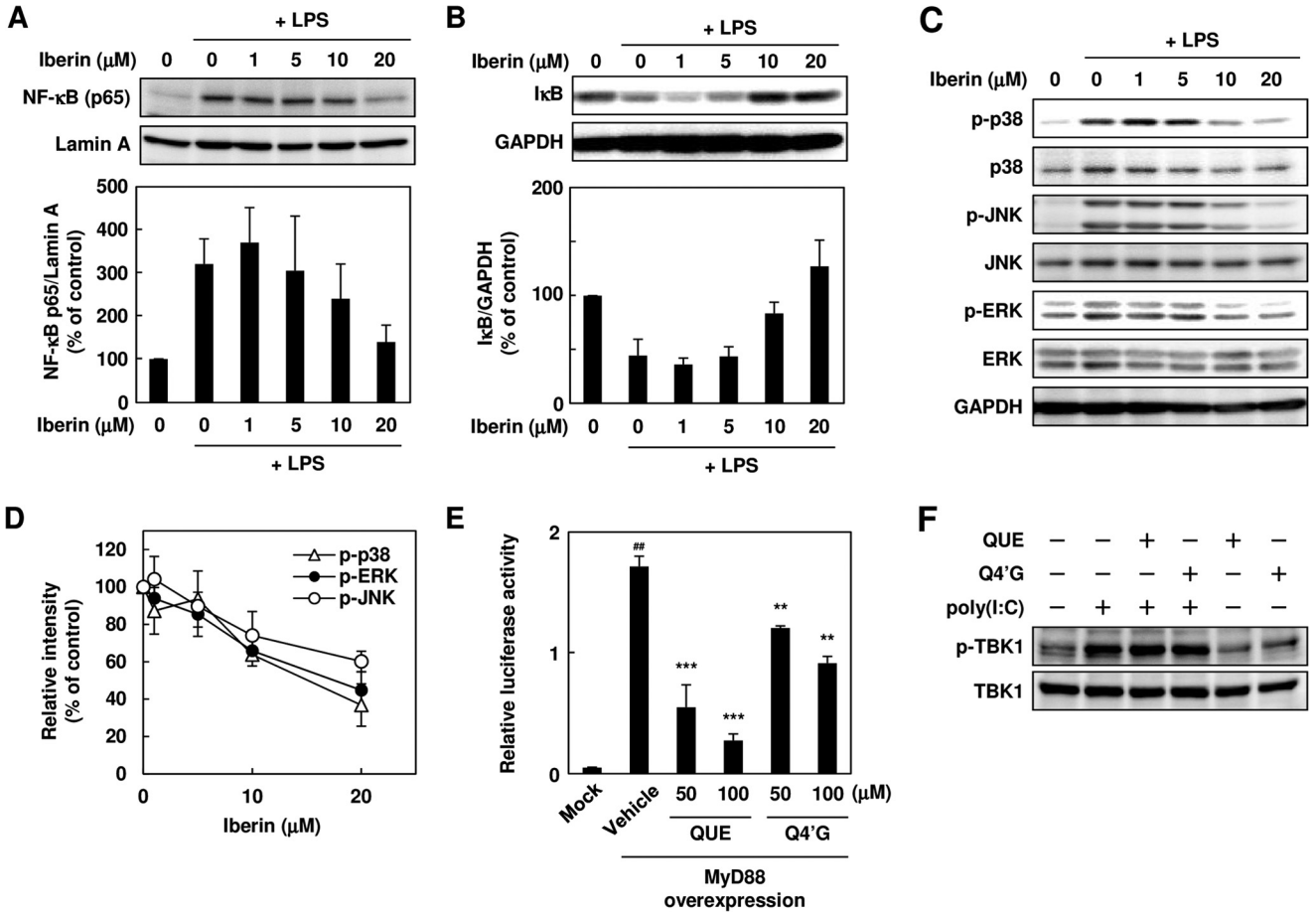

FIGURE 9. **Effect of iberin on NF-κB signaling pathway.** *A*, immunoblot analysis of nuclear translocation of p65. The RAW 264.7 cells were pretreated with iberin for 30 min and then treated with LPS (100 ng/ml) for 4 h. After incubation, the nuclear fractions were prepared, and immunoblotting was performed with the anti-p65 and anti-lamin A antibodies. A representative immunoblot (*top*) and densitometric analysis of p65 protein normalized to lamin A (*bottom*) are shown. *Error bars* represent S.D. *B*, immunoblot analysis of IκB degradation. The cells were pretreated with iberin for 30 min and then treated with LPS (100 ng/ml) for 30 min. After incubation, immunoblotting was performed with the anti-IκB and anti-GAPDH antibodies. A representative immunoblot (*top*) and densitometric analysis of IκB protein normalized to GAPDH (*bottom*) are shown. *Error bars* represent S.D. *C* and *D*, immunoblot analysis of phosphorylation of mitogen-activated protein kinases. The RAW264.7 cells were pretreated with iberin for 30 min and then treated with LPS (100 ng/ml) for 30 min. A representative immunoblot (*C*) and densitometric analysis of phosphorylated (*p-*) MAPKs normalized to total MAPKs (*D*) are shown. The values of LPS-treated cells are shown as a control (100%). *Error bars* represent S.D. *E*, effect of quercetin and Q4′G on NF-κB activation mediated by MyD88. The HEK293 cells were transiently co-transfected with the expression plasmid for the adaptor protein MyD88 or empty vector (*Mock*) and NF-κB reporter plasmid. After transfection, the cells were treated with quercetin (*QUE*) or Q4′G for 24 h. #, $p < 0.01$ *versus* Mock; ***, $p < 0.005$ and **, $p < 0.01$ *versus* vehicle (MyD88 expression). *Error bars* represent S.D. *F*, effect of quercetin and Q4′G on poly(I:C)-induced phosphorylation of TBK1 (*p-TBK1*). RAW264.7 cells were pretreated with quercetin or Q4′G (10 μM) for 30 min and then treated with poly(I:C) (10 μg/ml) for 30 min.

thiomethyl moieties showed no effect on the inhibitor potencies (*panels a* and *b*). In addition, an increase in the bulkiness of the alkylsulfinyl moiety resulted in no significant effects on the inhibitory activity (*panels c* and *d*). However, the inhibitor potency was influenced by the oxidation state of sulfur (*panels e* and *f*). Although the predicted molecular hydrophobicity (partition coefficients (log *P*)) was not statistically significant, these data are consistent with the sum of the surface contributions of polar atoms (polar surface area) (Fig. 12, *B–D*).

To gain more insight into the fundamental structural principles that govern the oxidation state of sulfur in the isothiocyanates and to relate the results to the experimental observations regarding their inhibitor potencies, we performed a computational analysis. The overlays of the conformers belonging to the same cluster are represented in Fig. 13. These overlays show that conformations that belong to the same cluster but have different energies essentially differ in the torsional angles of the thioether linkages (Fig. 13). Thus, the oxidation state of sulfur is likely to influence the global shape of the isothiocyanates, which might be associated with their inhibitory effects toward the TLR signaling.

DISCUSSION

In the present study, we screened extracts from a variety of commonly consumed vegetables and identified cabbage, onion, and beet as potential sources of anti-inflammatory substances. We selected cabbage and onion and attempted to identify the active substances and characterize the molecular mechanisms responsible for their anti-inflammatory effects. Cabbage is one of the most popular *Brassica* vegetables. Cabbage extracts have been reported to have a variety of biological activities, including anticarcinogenic properties (19, 20), suppression of hypercholesterolemia in hepatoma-bearing rats (21), and antiulcerogenic activity (22). Many of these beneficial effects of cabbages have been partly attributed to the high content of organosulfur compounds, including isothiocyanates (23). Onions also pro-

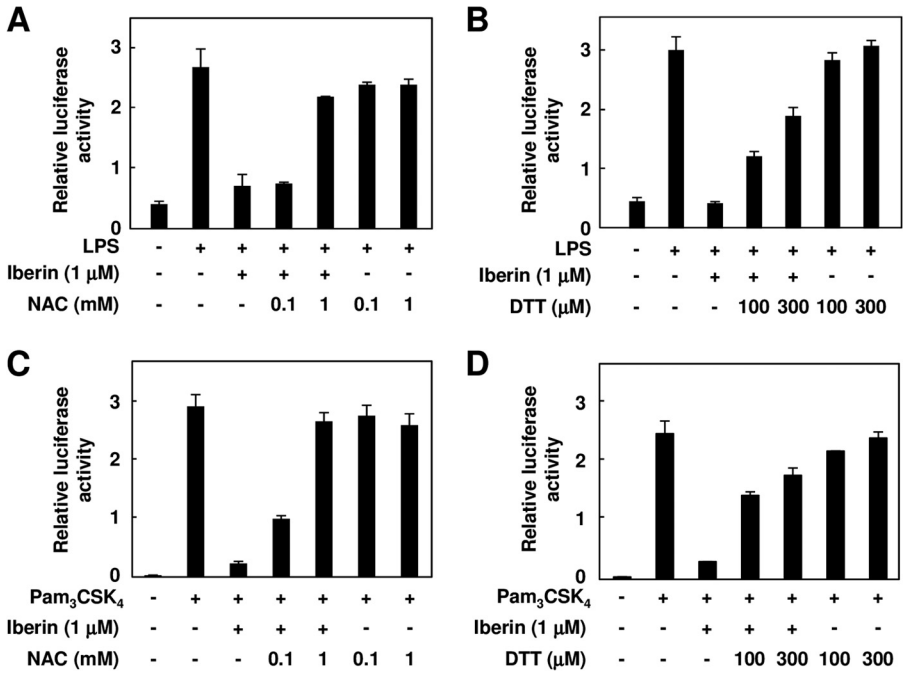

FIGURE 10. **Effect of thiol compounds on the TLR inhibition by iberin.** The HEK293-TLR4 (*A* and *B*) or HEK293-TLR2 (*C* and *D*) cells were pretreated with iberin (1 μM) in the presence of *N*-acetylcysteine (*NAC*) (*A* and *C*) or DTT (*B* and *D*) for 30 min and then treated with 100 ng/ml LPS (*A* and *B*) or Pam_3CSK_4 (*C* and *D*) for 24 h. *Error bars* represent S.D.

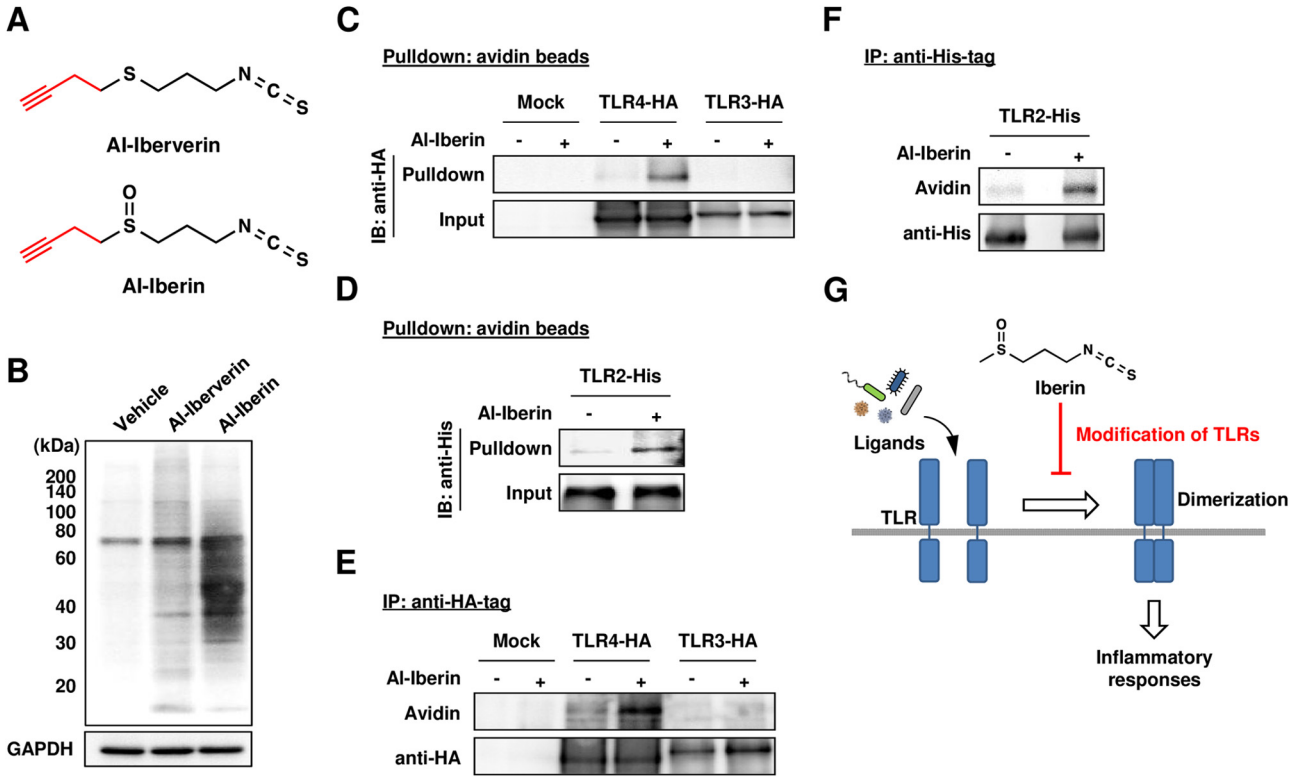

FIGURE 11. **Covalent modification of TLR4 by iberin.** *A*, chemical structures of Al-iberin and Al-iberverin. *B*, HRP-avidin detection of protein-bound iberin. The cells were pretreated with the alkynylated analogues (Al-iberin and Al-iberverin) or vehicle for 30 min. The cell lysates were subjected to the click reaction with biotin-N_3 followed by separation on an SDS-polyacrylamide gel and immunoblot analysis using HRP-avidin. *C*, the HEK293 cells transfected with TLR4-HA or TLR3-HA were treated with Al-iberin or vehicle (ethanol) for 30 min. The cell lysates were subjected to the click reaction with biotin-N_3, and the labeled proteins were precipitated with NeutrAvidin beads followed by Western blot with an anti-HA tag antibody. *D*, the HEK293 cells transfected with TLR2-His were treated with Al-iberin or vehicle (ethanol) for 30 min. The cell lysates were subjected to the click reaction with biotin-N_3, and the labeled proteins were precipitated with NeutrAvidin beads followed by Western blotting with an anti-His tag antibody. *E*, the HEK293 cells transfected with TLR4-HA or TLR3-HA were treated with Al-iberin or vehicle for 30 min. The cell lysates were subjected to the click reaction with biotin-N_3, and the labeled proteins were immunoprecipitated with an anti-HA tag antibody followed by Western blotting with an anti-HA tag antibody and HRP-avidin. *F*, the HEK293 cells transfected with TLR2-His were treated with Al-iberin or vehicle for 30 min. The cell lysates were subjected to the click reaction with biotin-N_3, and the labeled proteins were immunoprecipitated with an anti-His tag antibody followed by Western blotting with an anti-His tag antibody and HRP-avidin. *G*, proposed mechanisms by which iberin inhibits the ligand-induced TLR signaling. *IP*, immunoprecipitation; *IB*, immunoblotting.

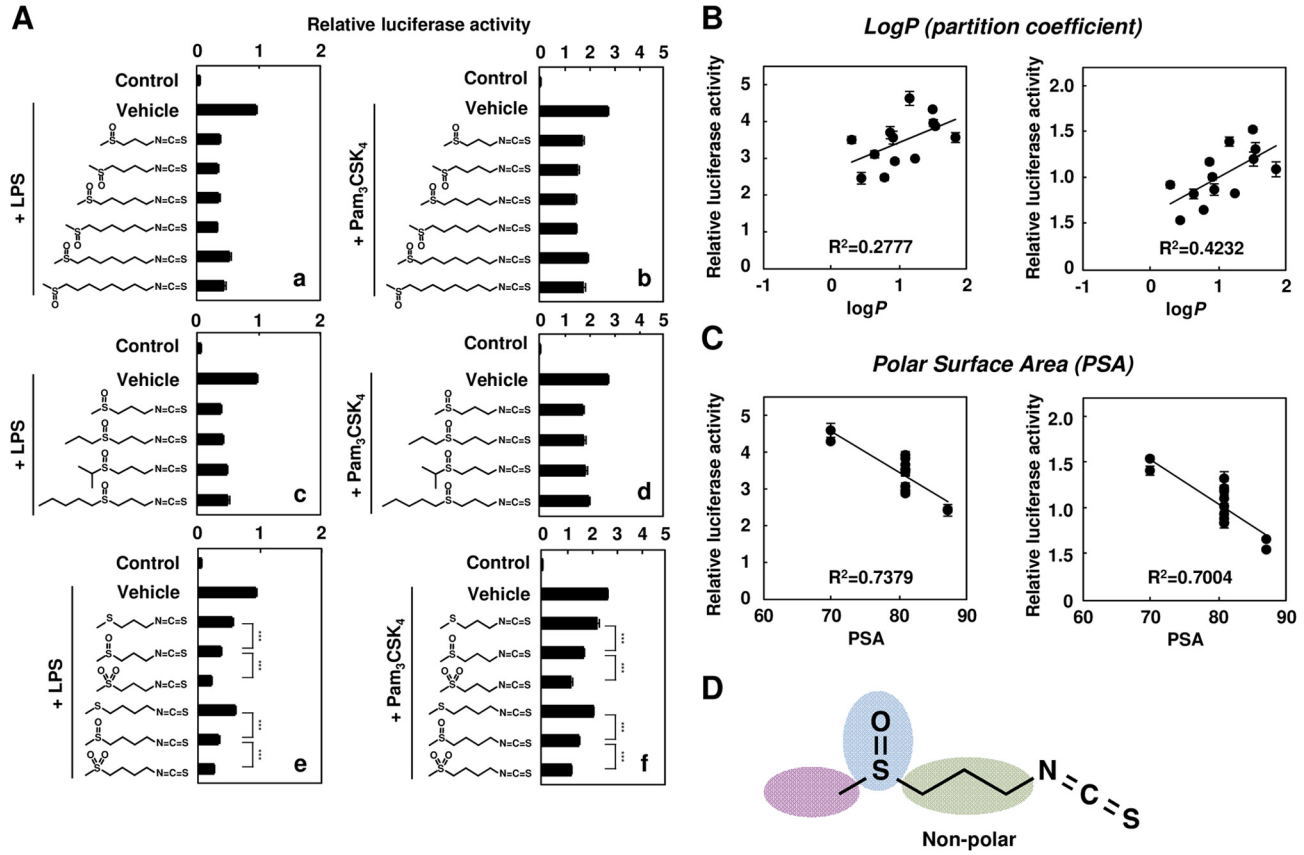

FIGURE 12. **Structure-activity relationship of isothiocyanate.** *A*, the HEK293-TLR4/MD2 cells (*panels a*, *c*, and *e*) or HEK293-TLR2 (*panels b*, *d*, and *f*) were pretreated with isothiocyanate derivatives (0.5 μM) for 30 min and then treated with 100 ng/ml LPS (*panels a*, *c*, and *e*) or Pam_3CSK_4 (*panels b*, *d*, and *f*) for 24 h. The results shown are means ± S.D. (*error bars*) of three independent experiments. ***, $p < 0.005$. *B*, correlation between log *P* and TLR2 (*left*) or TLR4 (*right*) inhibitory potency. log *P* was calculated using ChemBioDraw Ultra 12.0. *C*, correlation between polar surface area (*PSA*) and TLR2 (*left*) or TLR4 (*right*) inhibitory potency. Polar surface area was calculated using ChemBioDraw Ultra 12.0. *D*, iberin contains an isothiocyanate group, methylene groups, and alkylsulfinyl group.

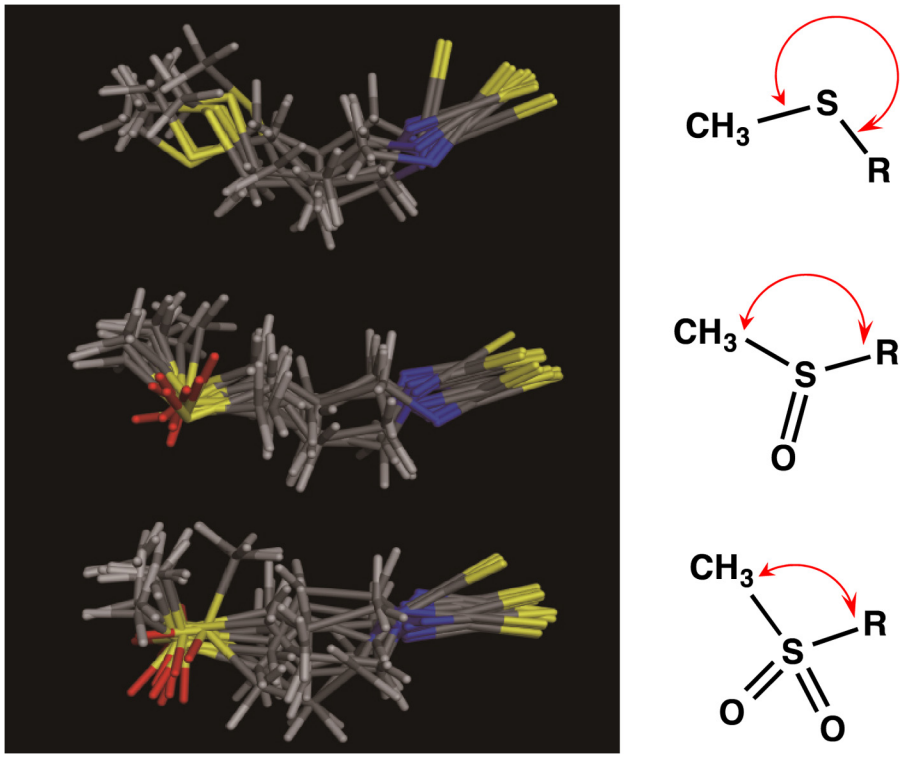

FIGURE 13. **The overlay of the 10 most stable conformations of iberin derivatives calculated by energy minimization.** *Top*, 3-methylthiopropyl isothiocyanate (iberverin); *middle*, 3-(methylsulfinylpropyl isothiocyanate (iberin); *bottom*, 3-methylsulfonylpropyl isothiocyanate (cheirolin). *Yellow*, sulfur; *blue*, nitrogen; *red*, oxygen.

vide important nutrients and health-promoting phytochemicals, including quercetin (24, 25).

The isothiocyanates are compounds that occur as glucosinolates in a variety of cruciferous vegetables, such as the *Brassica* species (26, 27). The glucosinolates are found in the cell vacuoles of various plants in the family Cruciferae, such as horseradish, broccoli, and cabbage. When plant cells are damaged, glucosinolates are hydrolyzed by myrosinase, which is also produced in the same family, and isothiocyanates are produced. Among the varieties of isothiocyanates, the ω-methylsulfinylalkyl isothiocyanates, such as 4-methylsulfinylbutyl isothiocyanate (sulforaphane), have attracted much attention. This class of isothiocyanates has been reported to have its own unique spectrum of biological effects, including the induction of phase 2 detoxification and antioxidant enzymes (28–30). They are also effective chemoprotective agents against chemical carcinogenesis in experimental animals, and several epidemiologic studies suggest that the consumption of cruciferous vegetables may be particularly effective in reducing the cancer risk at several organ sites (27). In the present study, we identified iberin, an analogue of sulforaphane, as one of the major TLR signaling inhibitors from cabbage (Fig. 3). Iberin glucosinolate (3-methylsulphinyl propyl glucosinolate; glucoiberin) has been isolated previously from the seeds of *Iberis amara* L. (31) and broccoli (32). There are few studies regarding iberin in comparison with sulforaphane. Iberin has been reported to induce cell cycle arrest and apoptosis in human neuroblastoma cells (33); increase glutathione *S*-transferase and quinone reductase activities in the urinary bladder of rats, demonstrating its protective effects against chemical carcinogenesis (34); and up-regulate the expression of thioredoxin reductase 1 in human MCF cells (35). However, as far as we know, the anti-inflammatory effects of iberin have not been investigated in detail.

Some phytochemicals with anti-inflammatory effects contain a structural motif that can react with the thiol group, a biological nucleophile, by the Michael addition reaction (36, 37). Given the critical importance of the NF-κB activity for the expression of proinflammatory genes, a number of studies have focused on the NF-κB pathway as the target of anti-inflammatory electrophilic compounds. Curcumin with an α,β-unsaturated carbonyl group inhibits NF-κB activation by interfering with IκB degradation and by reacting with the p50 subunit of the NF-κB complex through cysteine modification (38). In addition, sesquiterpene lactones react with cysteine residues in the p65 subunit of NF-κB, thereby inhibiting DNA binding of the NF-κB (39, 40).

TLRs are type I transmembrane receptors and possess several cysteine residues in both the extracellular and cytoplasmic domains that may form a disulfide linkage for the dimerization of the receptors (41). We found in this study that iberin could act on the TLR4 dimerization step, which is required to activate the downstream signaling pathway of TLR. These results and the fact that pretreatment with thiol-containing reagents DTT and *N*-acetylcysteine significantly suppressed the inhibitory potency of iberin (Fig. 10) suggested the possibility that electrophilic anti-inflammatory phytochemicals may react with the cysteine residue(s) of TLRs, leading to the inhibition of the TLR dimerization. Previous studies have shown that other electrophilic phytochemicals, such as curcumin, helenalin, and cinnamaldehyde, inhibit the LPS-induced dimerization of TLR4 (42, 43). Youn *et al.* (44) reported that sulforaphane inhibited TLR4 oligomerization. In addition, they analyzed the reaction of the purified extracellular domain of TLR4 with sulforaphane and concluded that sulforaphane formed adducts with the cysteine residue in the extracellular domain of TLR4. More recently, Koo *et al.* (45) showed that sulforaphane suppressed the engagement of LPS with the TLR4-MD2 complex through covalent modification of the cysteine residue of MD2. However, these findings are based on the *in vitro* studies using the purified peptides, and therefore direct evidence for the covalent binding of dietary phytochemicals to TLRs has not been obtained.

The modification of proteins is recognized as a key mechanism underlying the biological activity of isothiocyanates. The electrophilic carbon residue in the isothiocyanate moiety is capable of reacting with biological nucleophiles, such as cysteine in proteins. Binding of the isothiocyanates to cellular proteins, such as the transient receptor potential channels (46), has been demonstrated to occur via the covalent modification of cysteine. Using a click chemistry-based proteomic approach, Ahn *et al.* (47) have shown that sulforaphane is highly reactive with cysteine residues in proteins, such as Keap1, the macrophage migration inhibitory factor, and thioredoxin, to form covalent bonds. They have also shown that the reactive isothiocyanates of sulforaphane can be replaced by the more gentle electrophilic sulfoxythiocarbamate group that also selectively targets cysteine residues in proteins but forms stable thiocarbamate adducts. In the present study, to achieve the specific and efficient thiocarbamoylation of the target proteins by the isothiocyanates in intact cells, novel probes with an alkyne group, such as Al-iberin and Al-iberverin, were designed based on iberin (Fig. 11*A*). We introduced the alkyne rather than the azide functionality on the probe based on several chemical considerations indicated by Gillet *et al.* (48). Although azide-functionalized molecules seem compatible under *in vivo* labeling conditions (49), the chemical propensity of azides to undergo reduction into amines might be of concern. In addition, a significantly lower level of background labeling was obtained when the alkyne probe was used in combination with an azide fluorescent reporter. The presence of the alkyne functionality could then be detected in a later step upon the Cu(I)-catalyzed Huisgen [3 + 2] cycloaddition (click chemistry) reaction with an azide-functionalized fluorescent group (azide-rhodamine) (18). This approach enabled us to detect thiocarbamoylated proteins in the cells upon exposure to the isothiocyanate probes (Fig. 11*B*). We were unable to detect TLRs as the target of the isothiocyanate probes in the mass spectrometry-based proteomic study. This may be due to the relative abundance of the TLRs in the RAW264.7 cells. Instead of the proteomics identification, we confirmed the covalent binding of the iberin probe to TLR2 and TLR4, but not to the TLR3, by a pulldown assay (Fig. 11, *C–F*). These results suggest that covalent modification of the plasma membrane-located TLRs is involved in the disruption of the TLR dimerization (Fig. 11*G*). Although regulation of TLR dimerization and its significance need to be further confirmed *in vivo* in future studies, our *in vivo* studies demonstrated that the oral administration of iberin exhibited protective effects against

LPS-induced inflammatory responses (Fig. 5, *F* and *G*), suggesting that inhibitory effects of iberin on the TLR4 dimerization may result in anti-inflammatory responses *in vivo*.

Our click chemistry-based study showed that the electrophilic centers might be responsible for the anti-inflammatory effect of the isothiocyanate compounds. It has been suggested that the electrophilic potentials of various alkyl and aromatic isothiocyanates are dependent on the presence of one hydrogen on the carbon adjacent to the isothiocyanate group and that tautomerization of the methylene isothiocyanate moiety to a structure resembling an α,β-unsaturated thioketone may be important for their biological activities (50). Because iberin is structurally similar to sulforaphane, the TLR signaling inhibition potencies of iberin and sulforaphane were anticipated to be equally potent. Indeed, the structure-activity relationship study revealed that the inhibition potency of iberin was almost comparable with that of other methylsulfinylalkyl isothiocyanates (Fig. 12*A*). We also observed that the bulkiness of the alkylsulfinyl groups resulted in no significant effects on the inhibition potency and that the methylthioalkyl isothiocyanates were less potent inhibitors than their *S*-oxidized forms, suggesting that the hydrophilicity of the isothiocyanates may increase their inhibitory effect on the TLR signaling. Insight into the relationship between the oxidation state of sulfur in the isothiocyanates and their inhibition potencies was obtained from potential predictors of the intestinal permeability of the isothiocyanates (Fig. 12, *B* and *C*). In addition, the computational analysis also showed that the oxidation state of sulfur might change the torsional angles of the methylthioalkyl linkages, influencing the global shape of the isothiocyanates (Fig. 13). The methylsulfinyl group in addition to the isothiocyanate group of iberin is therefore suggested to be involved in its inhibition activity. Although the increased inhibition potency of the methylsulfinylalkyl and methylsulfonylalkyl isothiocyanates may be simply due to their low volatility, it is not unlikely that the electron-withdrawing potentials of both the sulfinyl and sulfonyl groups may also affect the inhibition potency.

We also found that onion is another rich source of inhibitors and identified not only quercetin but also its glucoside derivative as the TLR signaling inhibitors. It has been reported that quercetin exerts its anti-inflammatory effect through the inhibition of mitogen-activated protein kinases and NF-κB-mediated proinflammatory molecules such as cytokines, COX-2, and inducible nitric-oxide synthase (51, 52). However, in the present study, we found that both quercetin and Q4′G inhibited the TLR2 and TLR4 pathways (Fig. 7). In addition, they suppressed the activation of NF-κB induced by MyD88 overexpression (Fig. 9*E*), suggesting that these flavonoids may also act downstream of MyD88. Thus, the quercetin derivatives may affect multiple steps in the TLR4/NF-κB signaling pathway. Quercetin and Q4′G have no electrophilic groups to confer the Michael reaction. The biochemical mechanisms underlying the interaction of quercetin and its glucoside with TLR to exert inhibitory effects are therefore not completely understood.

Acknowledgment—We thank Dr. K. Miyake (University of Tokyo) for the kind gifts of pEFBOS-FLAGHis-mouse TLR4 and pEFBOS-FLAGHis-mouse MD2 vectors.

REFERENCES

1. Nathan, C. (2002) Points of control in inflammation. *Nature* **420,** 846–852
2. Barton, G. M. (2008) A calculated response: control of inflammation by the innate immune system. *J. Clin. Investig.* **118,** 413–420
3. Haddad, J. J., and Harb, H. L. (2005) L-γ-Glutamyl-L-cysteinyl-glycine (glutathione; GSH) and GSH-related enzymes in the regulation of pro- and anti-inflammatory cytokines: a signaling transcriptional scenario for redox(y) immunologic sensor(s)? *Mol. Immunol.* **42,** 987–1014
4. Takeda, K., and Akira, S. (2005) Toll-like receptors in innate immunity. *Int. Immunol.* **17,** 1–14
5. Takeuchi, O., and Akira, S. (2001) Toll-like receptors; their physiological role and signal transduction system. *Int. Immunopharmacol.* **1,** 625–635
6. Cohen, J. (2002) The immunopathogenesis of sepsis. *Nature* **420,** 885–891
7. Fujihara, M., Muroi, M., Tanamoto, K., Suzuki, T., Azuma, H., and Ikeda, H. (2003) Molecular mechanisms of macrophage activation and deactivation by lipopolysaccharide: roles of the receptor complex. *Pharmacol. Ther.* **100,** 171–194
8. Zhang, G., and Ghosh, S. (2001) Toll-like receptor-mediated NF-κB activation: a phylogenetically conserved paradigm in innate immunity. *J. Clin. Investig.* **107,** 13–19
9. Hantke, K., and Braun, V. (1973) Covalent binding of lipid to protein. Diglyceride and amide-linked fatty acid at the N-terminal end of the murein-lipoprotein of the *Escherichia coli* outer membrane. *Eur. J. Biochem.* **34,** 284–296
10. Zähringer, U., Lindner, B., Inamura, S., Heine, H., and Alexander, C. (2008) TLR2—promiscuous or specific? A critical re-evaluation of a receptor expressing apparent broad specificity. *Immunobiology* **213,** 205–224
11. Ness, A. R., and Powles, J. W. (1997) Fruit and vegetables, and cardiovascular disease: a review. *Int. J. Epidemiol.* **26,** 1–13
12. Sargeant, L. A., Khaw, K. T., Bingham, S., Day, N. E., Luben, R. N., Oakes, S., Welch, A., and Wareham, N. J. (2001) Fruit and vegetable intake and population glycosylated haemoglobin levels: the EPIC-Norfolk Study. *Eur. J. Clin. Nutr.* **55,** 342–348
13. Lee, J. Y., and Hwang, D. H. (2006) The modulation of inflammatory gene expression by lipids: mediation through Toll-like receptors. *Mol. Cells* **21,** 174–185
14. Halgren, T. A. (1996) Merck molecular force field. I. Basis, form, scope, parameterization, and performance of MMFF94. *J. Comp. Chem.* **17,** 490–519
15. Still, W. C., Tempczyk, A., Hawley, R. C., and Hendrickson, T. (1990) Semianalytical treatment of solvation for molecular mechanics and dynamics. *J. Am. Chem. Soc.* **112,** 6127–6129
16. Saitoh, S., Akashi, S., Yamada, T., Tanimura, N., Kobayashi, M., Konno, K., Matsumoto, F., Fukase, K., Kusumoto, S., Nagai, Y., Kusumoto, Y., Kosugi, A., and Miyake, K. (2004) Lipid A antagonist, lipid IVa, is distinct from lipid A in interaction with Toll-like receptor 4 (TLR4)-MD-2 and ligand-induced TLR4 oligomerization. *Int. Immunol.* **16,** 961–969
17. Ii, M., Matsunaga, N., Hazeki, K., Nakamura, K., Takashima, K., Seya, T., Hazeki, O., Kitazaki, T., Iizawa, Y. (2006) A novel cyclohexene derivative, ethyl (6R)-6-[N-(2-chloro-4-fluorophenyl)sulfamoyl]cyclohex-1-ene-1-carboxylate (TAK-242), selectively inhibits toll-like receptor 4-mediated cytokine production through suppression of intracellular signaling. *Mol. Pharmacol.* **69,** 1288–1295
18. Rostovtsev, V. V., Green, L. G., Fokin, V. V., and Sharpless, K. B. (2002) A stepwise Huisgen cycloaddition process: copper(I)-catalyzed regioselective "ligation" of azides and terminal alkynes. *Angew. Chem. Int. Ed. Engl.* **41,** 2596–2599
19. Komatsu, W., Miura, Y., and Yagasaki, K. (2002) Induction of tumor necrosis factor production and antitumor effect by cabbage extract. *Nutr. Cancer* **43,** 82–89
20. Mas, S., Crescenti, A., Gassó, P., Deulofeu, R., Molina, R., Ballesta, A., Kensler, T. W., and Lafuente, A. (2007) Induction of apoptosis in HT-29 cells by extracts from isothiocyanates-rich varieties of *Brassica oleracea*. *Nutr. Cancer.* **58,** 107–114

21. Komatsu, W., Miura, Y., and Yagasaki, K. (1998) Suppression of hypercholesterolemia in hepatoma-bearing rats by cabbage extract and its component, S-methyl-L-cysteine sulfoxide. *Lipids* **33,** 499–503
22. Carvalho, C. A., Fernandes, K. M., Matta, S. L., Silva, M. B., Oliveira, L. L., and Fonseca, C. C. (2011) Evaluation of antiulcerogenic activity of aqueous extract of *Brassica oleracea* var. *capitata* (cabbage) on Wistar rat gastric ulceration. *Arq. Gastroenterol.* **48,** 276–282
23. Stoewsand, G. S. (1995) Bioactive organosulfur phytochemicals in *Brassica oleracea* vegetables—a review. *Food. Chem. Toxicol.* **33,** 537–543
24. Vazquez-Prieto, M. A., and Miatello, R. M. (2010) Organosulfur compounds and cardiovascular disease. *Mol. Aspects. Med.* **31,** 540–545
25. Lee, J., and Mitchell, A. E. (2011) Quercetin and isorhamnetin glycosides in onion (*Allium cepa* L.): varietal comparison, physical distribution, coproduct evaluation, and long-term storage stability. *J. Agric. Food. Chem.* **59,** 857–863
26. Zhang, Y., and Talalay, P. (1994) Anticarcinogenic activities of organic isothiocyanates: chemistry and mechanisms. *Cancer Res.* **54,** 1976s-1981s.
27. Talalay, P., and Fahey, J. W. (2001) Phytochemicals from cruciferous plants protect against cancer by modulating carcinogen metabolism. *J. Nutr.* **131,** 3027S–3033S.
28. Zhang, Y., Talalay, P., Cho, C. G., and Posner, G. H. (1992) A major inducer of anticarcinogenic protective enzymes from broccoli: isolation and elucidation of structure. *Proc. Natl. Acad. Sci. U.S.A.* **89,** 2399–2403
29. Fahey, J. W., Zhang, Y., and Talalay, P. (1997) Broccoli sprouts: an exceptionally rich source of inducers of enzymes that protect against chemical carcinogens. *Proc. Natl. Acad. Sci. U.S.A.* **94,** 10367–10372
30. Morimitsu, Y., Nakagawa, Y., Hayashi, K., Fujii, H., Kumagai, T., Nakamura, Y., Osawa, T., Horio, F., Itoh, K., Iida, K., Yamamoto, M., and Uchida, K. (2002) A sulforaphane analogue that potently activates the Nrf2-dependent detoxification pathway. *J. Biol. Chem.* **277,** 3456–3463
31. Schults, O. E., and Gmelin, R. (1954) Mustard oil glycoside glucoiberine and bitter principle ibamarine of *Iberis amara* L. (candytuft). IX. Mustard oil glycoside. *Arch. Pharm. Ber. Dtsch. Pharm. Ges.* **287,** 404–411
32. Chuanphongpanich, S., Buddhasukh, D., Pirakitikulr, P., and Phanichphant, S. (2006) Analysis of intact glucosinolates in Thai broccoli seeds. *Chiang Mai J. Sci.* **33,** 223–230
33. Jadhav, U., Ezhilarasan, R., Vaughn, S. F., Berhow, M. A., and Mohanam, S. (2007) Iberin induces cell cycle arrest and apoptosis in human neuroblastoma cells. *Int. J. Mol. Med.* **19,** 353–361
34. Staack, R., Kingston, S., Wallig, M. A., and Jeffery, E. H. (1998) A comparison of the individual and collective effects of four glucosinolate breakdown products from brussels sprouts on induction of detoxification enzymes. *Toxicol. Appl. Pharmacol.* **149,** 17–23
35. Wang, W., Wang, S., Howie, A. F., Beckett, G. J., Mithen, R., and Bao, Y. (2005) Sulforaphane, erucin, and iberin up-regulate thioredoxin reductase 1 expression in human MCF-7 cells. *J. Agric. Food. Chem.* **53,** 1417–1421
36. Dinkova-Kostova, A. T., Massiah, M. A., Bozak, R. E., Hicks, R. J., and Talalay, P. (2001) Potency of Michael reaction acceptors as inducers of enzymes that protect against carcinogenesis depends on their reactivity with sulfhydryl groups. *Proc. Natl. Acad. Sci. U.S.A.* **98,** 3404–3409
37. Siedle, B., García-Piñeres, A. J., Murillo, R., Schulte-Mönting, J., Castro, V., Rüngeler, P., Klaas, C. A., Da Costa, F. B., Kisiel, W., and Merfort, I. (2004) Quantitative structure-activity relationship of sesquiterpene lactones as inhibitors of the transcription factor NF-κB. *J. Med. Chem.* **47,** 6042–6054
38. Brennan, P., and O'Neill, L. A. (1998) Inhibition of nuclear factor κB by direct modification in whole cells—mechanism of action of nordihydroguaiaritic acid, curcumin and thiol modifiers. *Biochem. Pharmacol.* **55,** 965–973
39. Rüngeler, P., Castro, V., Mora, G., Gören, N., Vichnewski, W., Pahl, H. L., Merfort, I., and Schmidt, T. J. (1999) Inhibition of transcription factor NF-κB by sesquiterpene lactones: a proposed molecular mechanism of action. *Bioorg. Med. Chem.* **7,** 2343–2352
40. García-Piñeres, A. J., Castro, V., Mora, G., Schmidt, T. J., Strunck, E., Pahl, H. L., and Merfort, I. (2001) Cysteine 38 in p65/NF-κB plays a crucial role in DNA binding inhibition by sesquiterpene lactones. *J. Biol. Chem.* **276,** 39713–39720
41. Tao, X., Xu, Y., Zheng, Y., Beg, A. A., and Tong, L. (2002) An extensively associated dimer in the structure of the C713S mutant of the TIR domain of human TLR2. *Biochem. Biophys. Res. Commun.* **299,** 216–221
42. Youn, H. S., Saitoh, S. I., Miyake, K., and Hwang, D. H. (2006) Inhibition of homodimerization of Toll-like receptor 4 by curcumin. *Biochem. Pharmacol.* **72,** 62–69
43. Youn, H. S., Lee, J. K., Choi, Y. J., Saitoh, S. I., Miyake, K., Hwang, D. H., and Lee, J. Y. (2008) Cinnamaldehyde suppresses toll-like receptor 4 activation mediated through the inhibition of receptor oligomerization. *Biochem. Pharmacol.* **75,** 494–502
44. Youn, H. S., Kim, Y. S., Park, Z. Y., Kim, S. Y., Choi, N. Y., Joung, S. M., Seo, J. A., Lim, K. M., Kwak, M. K., Hwang, D. H., and Lee, J. Y. (2010) Sulforaphane suppresses oligomerization of TLR4 in a thiol-dependent manner. *J. Immunol.* **184,** 411–419
45. Koo, J. E., Park, Z. Y., Kim, N. D., and Lee, J. Y. (2013) Sulforaphane inhibits the engagement of LPS with TLR4/MD2 complex by preferential binding to Cys133 in MD2. *Biochem. Biophys. Res. Commun.* **434,** 600–605
46. Macpherson, L. J., Dubin, A. E., Evans, M. J., Marr, F., Schultz, P. G., Cravatt, B. F., and Patapoutian, A. (2007) Noxious compounds activate TRPA1 ion channels through covalent modification of cysteines. *Nature* **445,** 541–545
47. Ahn, Y. H., Hwang, Y., Liu, H., Wang, X. J., Zhang, Y., Stephenson, K. K., Boronina, T. N., Cole, R. N., Dinkova-Kostova, A. T., Talalay, P., and Cole, P. A. (2010) Electrophilic tuning of the chemoprotective natural product sulforaphane. *Proc. Natl. Acad. Sci. U.S.A.* **107,** 9590–9595
48. Gillet, L. C., Namoto, K., Ruchti, A., Hoving, S., Boesch, D., Inverardi, B., Mueller, D., Coulot, M., Schindler, P., Schweigler, P., Bernardi, A., and Gil-Parrado, S. (2008) In-cell selectivity profiling of serine protease inhibitors by activity-based proteomics. *Mol. Cell. Proteomics* **7,** 1241–1253
49. Speers, A. E., Adam, G. C., and Cravatt, B. F. (2003) Activity-based protein profiling *in vivo* using a copper(I)-catalyzed azide-alkyne [3 + 2] cycloaddition. *J. Am. Chem. Soc.* **125,** 4686–4687
50. Talalay, P., De Long, M. J., and Prochaska, H. J. (1988) Identification of a common chemical signal regulating the induction of enzymes that protect against chemical carcinogenesis. *Proc. Natl. Acad. Sci. U.S.A.* **85,** 8261–8265
51. Wadsworth, T. L., and Koop, D. R. (1999) Effects of the wine polyphenolics quercetin and resveratrol on pro-inflammatory cytokine expression in RAW 264.7 macrophages. *Biochem. Pharmacol.* **57,** 941–949
52. Comalada, M., Ballester, I., Bailón, E., Sierra, S., Xaus, J., Gálvez, J., de Medina, F. S., and Zarzuelo, A. (2006) Inhibition of pro-inflammatory markers in primary bone marrow-derived mouse macrophages by naturally occurring flavonoids: analysis of the structure-activity relationship. *Biochem. Pharmacol.* **72,** 1010–1021